UNIVERSITAT ROVIRA I VIRGILI
DISEÑO DE CATALIZADORES PARA UNA OBTENCIÓN LIMPIA DE 2-FENILETANOL
Olga Bergadà Miró
ISBN:978-84-691-0355-5/DL:T.2186-2007

4. RESULTS AND DISCUSSION

4.1 Ni and Ni-MgO catalytic systems

4.1.1 Introduction

The properties of nickel oxide, as precursor of Ni catalysts, have been widely studied [47-49]. Systems containing Ni are know to be active catalysts in hydrogenation reactions due to the ability of metallic nickel to chemisorb dissociatively molecular hydrogen [50,51]. The Raney-Ni catalyst, first synthesized at thirties [52], is one of the most used hydrogenation catalysts at industrial level due to its high metallic area, and its great versatility to be used at low hydrogen pressures as well as under more vigorous conditions.

Taking into account that the properties of metallic catalysts are related to their catalytic activity, we have found many studies focused in the obtention of nickel oxides with different properties by using different preparative methods. Thus, nickel oxides with different degrees of crystallinity, particle sizes [53], morphologies [54] and specific surface areas have been prepared [55,56]. One of the most used NiO preparation methods is the decomposition of nickel nitrate hexahydrate [54,57,58]. These works report that when using thermal treatment with an efficient reduction of the residual water pressure on the sample, only decomposition products such as the dehydration nickel nitrates (tetrahydrate, dihydrate and the anhydrous samples) are obtained in the first steps. In contrast, the presence of water over the sample produces simultaneously dehydration and hydropyrolitic reactions causing the formation of basic nickel nitrates such as $2Ni(NO_3)_2Ni(OH)_2$ and $Ni(NO_3)_2Ni(OH)_2$. The physisorption study of the samples obtained at several temperatures and residual pressure conditions suggests the presence of intermediate compounds with different characteristics, which give place to NiO samples with different surface properties. Thus, the NiO obtained from nickel nitrate anhydrous has much higher area (about 50 m^2/g)

than the NiO formed by decomposition in stationary air (about 1 m^2/g) using a basic nitrate as a precursor [57].

In previous studies made in our research group, we observed that a careful decomposition of nickel nitrate hexahydrate until the formation of $Ni_3(NO_3)_2(OH)_4$ as a single phase, and subsequently calcination of this intermediate to form NiO, led to very homogeneous octahedral NiO particles [54].

MgO is a well-known basic solid [59]. Different Mg-O pairs exist at the surface of MgO, where Mg^{2+} and O^{2-} ions have different coordination numbers depending on their location (terrace, corner or edge). The stronger basic sites are generally considered to be oxide ions of low coordination [60]. Another characteristic of MgO is its great tendency to hydration.

Thus, NiO-MgO materials constitute a very interesting system since, after reduction, a Ni metallic catalyst with basic properties is obtained. This catalyst has been used in several reactions such as steam reforming of light hydrocarbons [61], hydrogenation of nitriles [62,63], isomerization of double bonds [64] and hydrogenation of ketones [65,66].

NiO-MgO systems have a tendency to form NiO-MgO solid solutions due to facile diffusion of Ni ions into the MgO support. Many studies have related the reducibility of the NiO-MgO systems with the catalytic performance of the corresponding Ni catalysts [67-69]. Other studies show the striking differences in the reactivity between the NiO formed on the MgO surface and the Ni ions dispersed into the MgO lattice [70]. It has been reported that the interaction of Ni ions with MgO has a positive effect on the resistance to coking, [71] whereas the strong interaction resulting from the high dispersion of Ni ions often lowers the reactivity of catalysts since the strong interaction depresses the formation of the active reduced Ni sites [72]. Therefore, the catalytic performance and reducibility of NiO-MgO systems are very influenced by the preparation conditions [73,74,75].

As commented in the introduction, bulk nickel, palladium and platinum catalysts have shown to be good catalysts for the catalytic hydrogenation of

UNIVERSITAT ROVIRA I VIRGILI
DISEÑO DE CATALIZADORES PARA UNA OBTENCIÓN LIMPIA DE 2-FENILETANOL
Olga Bergadà Miró
ISBN:978-84-691-0355-5/DL:T.2186-2007

styrene oxide to 2-phenylethanol [34,36]. Their activity and selectivity were considerably improved with the addition of basic solutions to the reaction medium (88% of selectivity to 2-phenylethanol for a 95% of conversion for a Raney-Ni catalyst) [34]. From these results, Mitsui et al. proposed that this basic reaction medium decreases the interaction between the oxygen of styrene oxide and the catalytic surface minimizing the ethylbenzene formation, and favouring the obtention of 2-phenylethanol (Esquema 7, pg 12).

Taking into account the good results found by using a Raney-Ni catalyst [34,36], we want to study the influence of the surface properties of differently prepared bulk nickel catalysts on the reaction, and also verify the effect of adding basicity to the reaction medium by introducing a solid with basic properties, as magnesia, in the nickel catalyst. The aim of this work is the preparation, characterization and study the catalytic activity for the styrene oxide hydrogenation of three bulk nickel catalysts with different morphologies, and several Ni-MgO systems. In these Ni-MgO systems, we modified the following parameters: a) the basic solid used (commercial magnesia (MgO) and rehydrated magnesia (MgOr)), b) the metallic nickel amount, and c) the distribution of basic and nickel sites by using two preparative methods. The catalytic results will be compared with a commercial Raney-Ni catalyst tested at the same reaction conditions. Moreover, the catalytic behaviour of the Ni-MgO systems will be correlated with CO_2-TPD studies.

4.1.2 Experimental

Catalysts preparation

Table 1 shows the preparation conditions of the different catalytic precursors. The structural differences of the bulk nickel catalysts were obtained by varying the preparation procedure of the NiO precursor through different decomposition ways of $Ni(NO_3)_2 6H_2O$.

Table 1. Preparation conditions of the catalytic precursors.

Catalytic precursor	Calcination temperature (K)	Direct precursor of NiO	NiO:MgO weight ratio
NiOA	553	$Ni(NO_3)_2$	-
NiOB	593	$Ni(NO_3)_2$	-
NiOC	593	$Ni_3(NO_3)_2(OH)_4$	-
NiOMgO	593	$Ni(NO_3)_2$	1:1
4NiOMgO	593	$Ni(NO_3)_2$	4:1
NiOMgOr	593	$Ni(NO_3)_2$	1:1
4NiOMgOr	593	$Ni(NO_3)_2$	4:1

Commercial $Ni(NO_3)_2 6H_2O$ (Panreac, 99%) was thermally decomposed, flowing Ar through the sample, at 453 K (about 6h) until $Ni(NO_3)_2$ was obtained as single phase. This was later calcined at 553 K for 6h to obtain the sample NiOA or at 593 K for 6h to obtain the sample NiOB. When the decomposition of $Ni(NO_3)_2 6H_2O$ was made at 393 K in an air static system, to maintain a certain water steam pressure on the sample, the product obtained after 14 days as single phase was the basic salt $Ni_3(NO_3)_2(OH)_4$. This salt was then calcined, flowing Ar through the sample, at 593 K for 6h to obtain the catalytic precursor NiOC.

NiO/MgO and NiO/MgO systems were obtained with different weight ratios (1:1 and 4:1) from physical mixtures of the NiOB samples (previoulsy prepared) with commercial magnesia (Aldrich, 99%) (MgO), or rehydrated magnesia (MgOr), respectively, by stirring the mixture in cyclohexane for 1 hour at room temperature. Rehydrated magnesia (MgOr) was prepared by refluxing commercial MgO in distilled water for 1 h. Then the solid was filtered and dried at 393 K overnight. The organic solvent was then evaporated. These catalytic precursors were named as NiOMgO, 4NiOMgO, NiOMgOr and 4NiOMgOr.

UNIVERSITAT ROVIRA I VIRGILI
DISEÑO DE CATALIZADORES PARA UNA OBTENCIÓN LIMPIA DE 2-FENILETANOL
Olga Bergadà Miró
ISBN:978-84-691-0355-5/DL:T.2186-2007

The reduction of the catalytic precursors to obtain the corresponding catalysts, NiA, NiB, NiC, NiMgO, 4NiMgO, NiMgOr and 4NiMgOr was made with pure H_2 at 523 K for 4 h. Other two catalysts, with Ni/MgO ratios of 1:1 and 4:1 (catalysts NiMgOa, 4NiMgOa), were prepared from physical mixtures of commercial MgO with metallic NiB by stirring in degassed cyclohexane at room temperature for 1hour and later evaporation of the solvent.

The Raney-nickel catalyst used was a commercial nickel sponge suspension in water (Fluka, 99%) and was dried under pure H_2 flow at 453 K for 1h (referred to as Raney-Ni).

Air-free sampling

The catalysts were always handled under air-free conditions after the reduction step. The catalysts were transferred in degassed cyclohexane and under a hydrogen atmosphere at room temperature. The cyclohexane surface-impregnated samples were further isolated from the air with sticky tape for XRD monitoring, where a glove box was used for mounting.

Characterization of the samples

The catalytic precursors and the catalysts were characterized by Infrared Spectroscopy, X-Ray Diffraction (XRD), BET areas, Temperature-programmed reduction (TPR), Scanning electron microscopy (SEM), Temperature-programmed desorption-mass spectrometry experiments (CO_2-TPD) and Hydrogen Chemisorption. The experimental conditions used have been indicated in the Experimental Section (3.2).

Catalytic activity determination

The catalytic hydrogenation of styrene oxide was made in the liquid phase, using for all tests 0.5 g of active phase, 20 mL of absolute ethanol (Panreac, 99.5%) and 4 mmol of styrene oxide (Aldrich, 97%) with a hydrogen flow of 2 ml/s and agitation of 700 rpm. The reaction was performed at room temperature, and at 323 K. Sample was taken each 1, 3 and 6 h. The reaction

products were analyzed by gas chromatography, using a chromatograph Shimadzu GC-2010 with 30 m of capillary column "DB-1" and a FID detector. They were quantified by adding internal standard and by using a calibrated line. We also tested the catalytic lifetime of the best catalyst by reusing the catalyst five times at the same catalytic conditions.

4.1.3 Results and discussion

Characterization of the catalytic precursors and catalysts

The rehydrated sample (MgOr) was characterized by infrared spectroscopy in order to determine the presence of hydroxyl groups. Fig.6 shows the IR spectrum for this sample where an intense band appeared at 3698 cm^{-1}, corresponding to hydroxyl groups, indicates the rehydration of magnesia. XRD pattern of MgOr (not shown here) confirms the complete transformation of periclase to brucite ($Mg(OH)_2$) after the rehydration process.

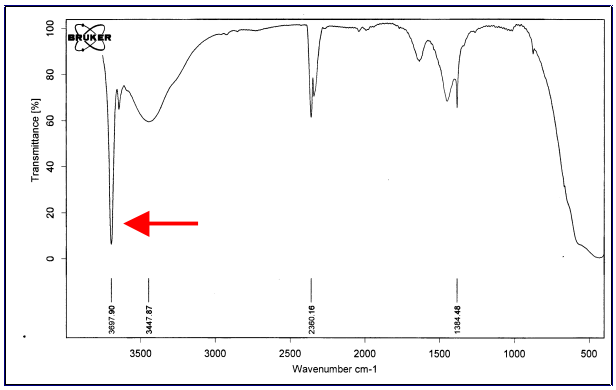

Figure 6. Infrared spectrum of rehydrated magnesia.

Table 2 shows several characterization data for the catalytic precursors. Powder diffraction patterns of the bulk NiO precursors exhibit five sharp peaks, which correspond to the crystalline NiO phase, whereas the NiO-MgO and NiO-MgOr systems show the expected NiO and MgO phases, and NiO and $Mg(OH)_2$ phases, respectively. The presence of two phases indicates that

UNIVERSITAT ROVIRA I VIRGILI
DISEÑO DE CATALIZADORES PARA UNA OBTENCIÓN LIMPIA DE 2-FENILETANOL
Olga Bergadà Miró
ISBN:978-84-691-0355-5/DL:T.2186-2007

there is not solid solution in none of these catalytic precursors and, therefore, NiO-MgO and NiO-$Mg(OH)_2$ interactions are low [75].

Table 2. Characterization of the catalytic precursors.

Catalytic precursors	Crystalline phases (XRD)	BET area (m^2/g)	NiO crystallite size (nm)[a]	Initial reduction tempetature[c] (K)
NiOA	NiO	64	12.9	581
NiOB	NiO	43	23.3	619
NiOC	NiO	55	31.8	611
NiOMgO	NiO, MgO	93	23.2[b]	644
4NiOMgO	NiO, MgO	67	23.5[b]	627
NiOMgOr	NiO, $Mg(OH)_2$	56	23.3[b]	636
4NiOMgOr	NiO, $Mg(OH)_2$	48	23.3[b]	621

[a] Using the Scherrer equation.[b] Calculated for the NiO phase.[c] Initial reduction temperature obtained from TPR experiments

Regarding the NiO precursors, sample NiOA has the highest BET area (64 m^2/g) and the smallest crystallite size (12.9 nm), as expected. Sample NiOB has lower surface area (43 m^2/g) and larger crystallite size (23.3 nm) than NiOA. This can be related to a greater sintering of the particles of this sample, which was calcined at higher temperature (593 K). This justifies a higher diffraction domain and its lower surface area. On the other hand, NiOC has an intermediate BET area (55 m^2/g) whereas its crystallite size is higher (31.8 nm) than those of the other samples. Taking into account that NiOC was calcined at 593 K (as NiOB), these values can be explained by the different characteristics of its corresponding precursor (Table 1), which gives place to a less crystalline NiO phase with a higher diffraction domain.

The BET area values observed for the MgO and MgOr samples are 130 and 73 m^2/g, respectively. Ni-MgO and Ni-MgOr precursors have BET area values proportional to the amount of added magnesia. Thus, the sample with higher magnesia content (NiOMgO) has the highest surface area (Table 2). The precursors with MgOr show lower surface areas than the precursors with commercial MgO (Table 2). These results were expected due to the lower surface area of the MgOr sample. Taking into account that the average crystallite size for the NiOB sample is 23.3 nm and for the commercial MgO

and sample MgOr are 16.9 nm and 19.4 nm, respectively, we observe that the NiOB average crystallite sizes obtained for the Ni-MgO and Ni-MgOr precursors did not practically change during the mixture process (Table 2).

In order to test the reducibility of the nickel oxides and to obtain more information about the NiO-MgO interaction, several temperature-programmed reduction studies were performed. From each plot, the initial reduction temperature (just when the reduction of NiO starts) was determined. The results are shown in Table 2.

The initial reduction temperature observed for the different NiO samples can be related to their surface area values. A higher surface area involves a lower initial reduction temperature. Thus, NiOA, with the highest surface area, starts to reduce before than the other NiO samples (NiOB and NiOC) (Table 2). NiO-MgO and NiO-MgOr systems show higher initial reduction temperature than its NiO precursor (NiOB) being the samples with commercial magnesia those that have higher initial reduction temperature values (Table 2). These results let us to think that there is a certain interaction between NiO and MgO, and between NiO and $Mg(OH)_2$, respectively. This interaction is slightly higher for the catalytic precursors with commercial magnesia. Thus, the system with higher amount of commercial magnesia (NiMgO) presents the highest initial reduction temperature (Table 2).

Scanning electron microscopy was used to monitor the morphology of the particles for the different catalytic precursors (Fig.7). The presence of particles which remind the octahedral morphology was observed for all of the NiO precursors (Figs.7a, 7b and 7c) but it is important to remark the lack of homogeneity in the particle sizes of the precursors NiOA (Fig.7a) and NiOB (Fig.7b). Sample NiOA has particle sizes between 1000 and 4000 Å whereas sample NiOB exhibits particle sizes in the range 1000-8000 Å. On the other hand, sample NiOC (Fig.7c) shows more defined octahedral particles with homogeneous size (1500 Å). This can be related to the use of $Ni_3(NO_3)_2(OH)_4$ as direct precursor of NiOC, as observed in previous work [53].

UNIVERSITAT ROVIRA I VIRGILI
DISEÑO DE CATALIZADORES PARA UNA OBTENCIÓN LIMPIA DE 2-FENILETANOL
Olga Bergadà Miró
ISBN:978-84-691-0355-5/DL:T.2186-2007

All the precursors prepared NiOB with commercial magnesia or with rehydrated magnesia show some particles with a certain octahedral morphology that should correspond to NiOB (Fig.7d, 7e). Additionally, the samples with MgOr exhibit particles with lamellar morphology corresponding to the brucite phase (Fig. 7e).

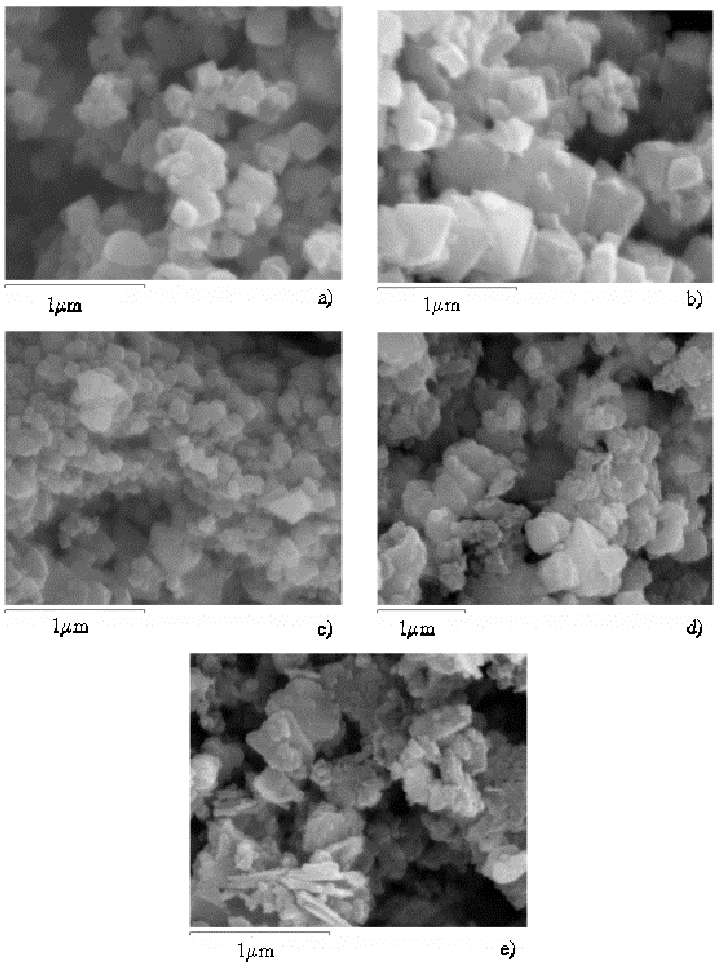

Figure 7. Scanning electron micrographs taken from the surface of the catalytic precursors: a) NiOA, b) NiOB, c) NiOC, d) NiOMgO, e) NiOMgOr.

Table 3 shows some characterization data of the prepared catalysts. Once reduced, as observed by XRD, all NiO is converted to crystalline metallic

nickel for all catalysts together with the corresponding MgO or $Mg(OH)_2$ phase for the Ni-MgO and Ni-MgOr catalysts, respectively. Catalyst NiB has the highest metallic area. The best reducibility of the catalytic precursors NiOA and NiOC, as deduced from TPR data, seems to favour a greater sintering of their nickel particles formed under the same reduction conditions than NiB.

Table 3. Characterization of the catalysts.

Catalyst	Crystalline phases (XRD)	% Ni	Metallic area (m^2/g sample)
NiA	Ni	100	0.5
NiB	Ni	100	1.7
NiC	Ni	100	0.6
NiMgO	Ni, MgO	44	0.9
4NiMgO	Ni, MgO	76	0.6
NiMgOr	Ni, $Mg(OH)_2$	44	0.4
4NiMgOr	Ni, $Mg(OH)_2$	76	0.2
NiMgOa	Ni, MgO	44	0.9
4NiMgOa	Ni, MgO	76	1.2

For the catalysts with MgOr (NiMgOr and 4NiMgOr) and for the catalyst 4NiMgO, we observe lower metallic areas than for catalyst NiB and for the catalysts prepared by mixing NiB with MgO (NiMgOa, 4NiMgOa). This can be related to the water formed during the reduction process that should give to some agglomeration of the periclase or brucite particles due to the hygroscopic properties of these basic compounds [64,75]. This involves, indirectly, a sintering of the metallic particles. For the samples with MgOr, their lower metallic area could be explained by a higher agglomeration due to the additional water formed by dehydroxylation of the surface hydroxyl groups. For the catalyst NiMgO, lower agglomeration and, consequently, higher metallic area can be expected, due to the more efficient water removing in this system, which presents lower reducibility (Table 2). Not

UNIVERSITAT ROVIRA I VIRGILI
DISEÑO DE CATALIZADORES PARA UNA OBTENCIÓN LIMPIA DE 2-FENILETANOL
Olga Bergadà Miró
ISBN:978-84-691-0355-5/DL:T.2186-2007

significant variations in the morphology of the NiO particles after reduction were observed by SEM.

The commercial Raney-Ni was characterized by H_2 chemisorption and SEM techniques. This catalyst has the highest metallic area (30 m^2/g) and, in contrast to the other catalysts, presents very amorphous nickel particles.

Basicity study of the catalytic precursors and catalysts by CO_2-TPD

In order to characterize the basic properties of the catalytic precursors with magnesia, NiOB, and their corresponding catalysts, the strength distribution of their basic sites were determined by TPD-MS of preadsorbed carbon dioxide.

Fig.8 shows the CO_2-TPD profiles of commercial MgO, sample NiOB and the catalytic precursors 4NiOMgO and NiOMgO.

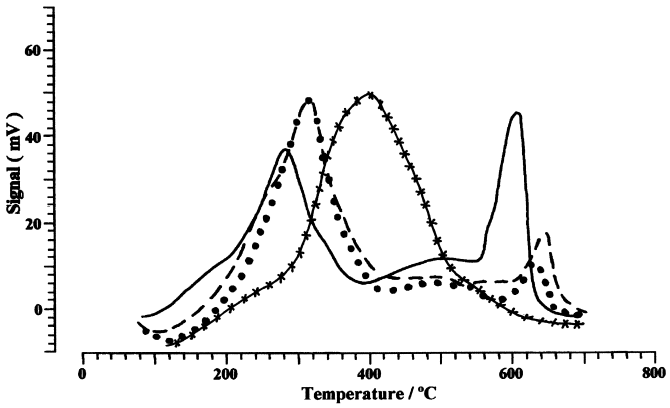

Figure 8. CO_2-TPDs of the samples: MgO(_), NiO (xxxx), 4NiOMgO (••••) and NiOMgO (----).

The TPD profile of commercial MgO mainly shows two intense desorption peaks at 280ºC and at 600ºC whereas the TPD profile of the NiO sample only shows one desorption peak around 420ºC. For the 4NiOMgO and NiOMgO precursors obtained by physical mixing of the NiOB sample and

commercial MgO in the appropriate amounts, we can observe two desorption peaks with different intensity and position respect to the peaks of the TPDs of commercial MgO and sample NiOB. This could be explained taking into account the NiOB/MgO ratio of the catalytic precursors and the existence of some interaction between NiOB and MgO.

Fig. 9 shows the CO_2-TPD profiles of rehydrated MgO (MgOr), the catalytic precursors NiOMgOr and 4NiOMgOr, and also of the NiOB sample for comparison.

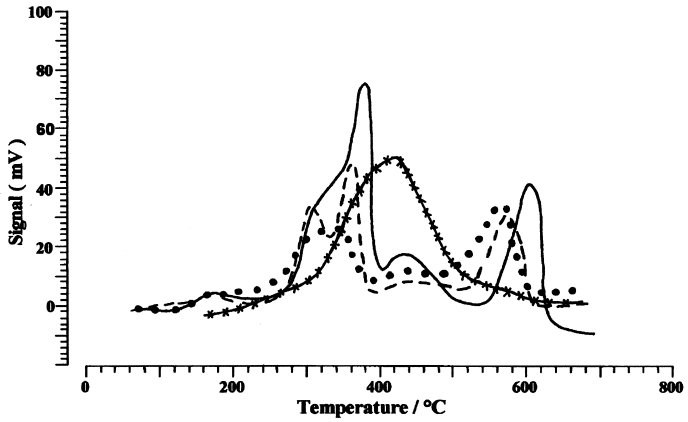

Figure 9. CO_2-TPDs of the samples: MgOr (_), NiO (xxxx), 4NiOMgOr (••••) and NiOMgOr (----).

The TPD profile of sample MgOr exhibits four desorption peaks: a medium-intense peak around 300ºC, which is a shoulder of the highest-intense peak appeared at 390ºC, a very low intense peak at 440ºC, and a peak with medium intensity at 600ºC. The catalytic precursors 4NiOMgOr and NiOMgOr show some changes in the position and intensity of the desorption peaks respect to the MgOr and NiOB TPDs. Again, the different NiOB/MgOr ratio and the presence of some NiOB/$Mg(OH)_2$ interaction could explain these results.

Fig. 10a shows the CO_2-TPD profile of catalyst NiMgO. The peaks in this thermogram have been assigned by comparison with the thermogram of

UNIVERSITAT ROVIRA I VIRGILI
DISEÑO DE CATALIZADORES PARA UNA OBTENCIÓN LIMPIA DE 2-FENILETANOL
Olga Bergadà Miró
ISBN:978-84-691-0355-5/DL:T.2186-2007

commercial MgO (Fig.8) and the thermogram obtained for the Ni sample without MgO (Fig 10b).

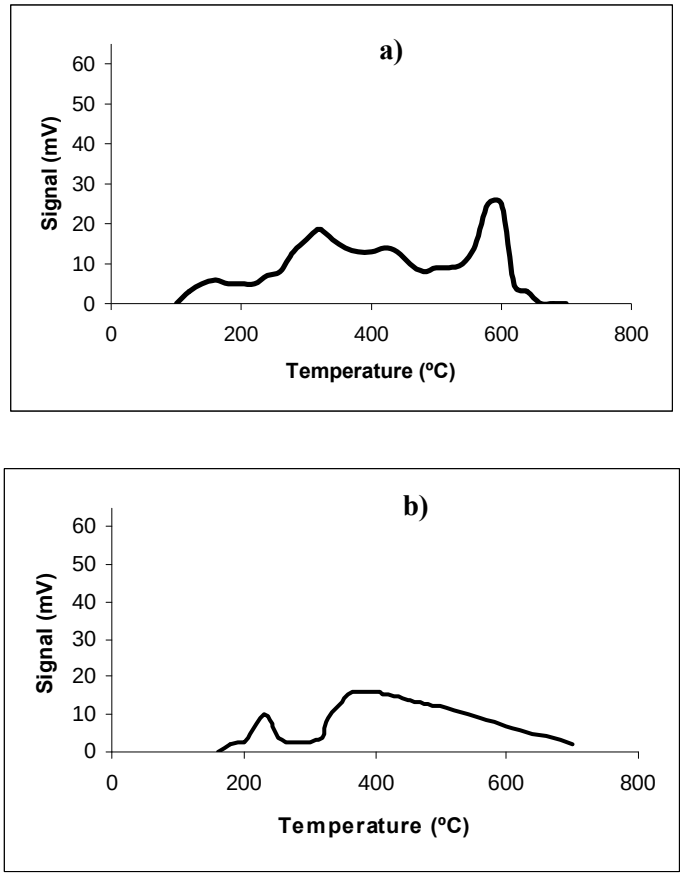

Figure 10. a) CO_2-TPD of the catalyst NiMgO; b) CO_2-TPD of the NiB catalyst.

In the TPD profile of the NiMgO catalyst, we can mainly see two desorption peaks: one with low intensity at 330ºC, which can be assigned by intensity and position to metallic nickel (see Fig.10b), and a peak with medium intensity at 600ºC which can be related to the stronger basic sites of magnesia (see Fig.8). When compared with the CO_2-TPD profile of MgO, we observe that the intense peak at 280ºC, corresponding to the weakest basic sites of commercial magnesia, now does not appear. This fact, together with the presence of the desorption peak characteristic of metallic nickel let us to

think that the metallic nickel particles formed by the NiOB reduction should cover the weakest basic sites of MgO in catalyst NiMgO, explaining the disappearance of this peak. These results suggest the existence of some interaction between the nickel and the weakest basic sites of magnesia. As it has been reported by other authors, CO_2 interacts with nickel being this interaction weaker when the nickel sites increase their electronic density in the presence of other oxide species [76]. This could explain the shift of the CO_2 desorption peak assigned to Ni sites at lower temperatures in the TPD of NiMgO (330ºC) respect to the same peak observed in the TPD of the NiB sample (370ºC). Lastly, the peak desorbed at 600 ºC (Fig.10a) has similar intensity and similar desorption temperature to that of commercial magnesia (Fig.8) taking into account the different MgO amount present in the two samples. This means that NiB particles do not interact practically with the stronger basic sites of magnesia.

Fig. 11 shows the CO_2-TPD profile of catalyst NiMgOr.

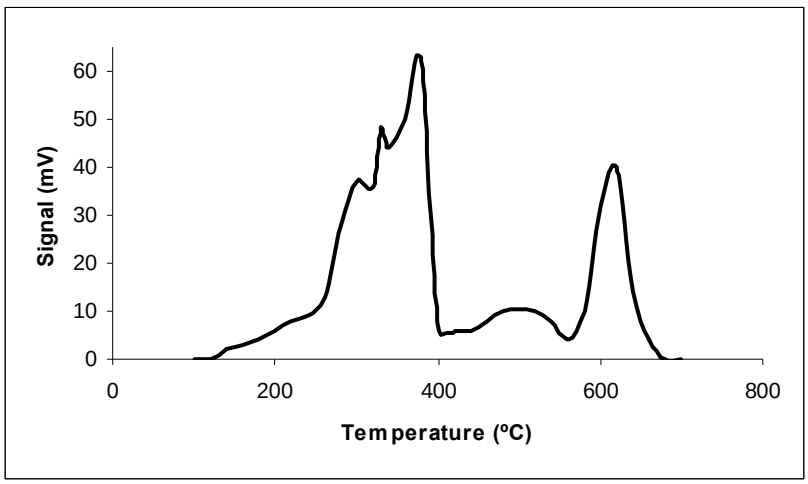

Figure 11. CO_2-TPD of the catalyst NiMgOr.

For the catalysts with rehydrated magnesia, the CO_2-TPD profiles are very similar to that of the rehydrated magnesia (Fig.9). However, a new peak appears around 340 ºC (between the peaks at 300ºC and 390ºC observed for

UNIVERSITAT ROVIRA I VIRGILI
DISEÑO DE CATALIZADORES PARA UNA OBTENCIÓN LIMPIA DE 2-FENILETANOL
Olga Bergadà Miró
ISBN:978-84-691-0355-5/DL:T.2186-2007

MgOr). This could be related to nickel sites interacting with basic sites or to basic sites of $Mg(OH)_2$ which are covering some nickel particles. Both situations involve a certain interaction between the Ni and the brucite particles.

Lastly, the CO_2-TPD profile of NiMgOa catalyst presents three desorption peaks at 280ºC, 370ºC, and 620ºC (Fig. 12).

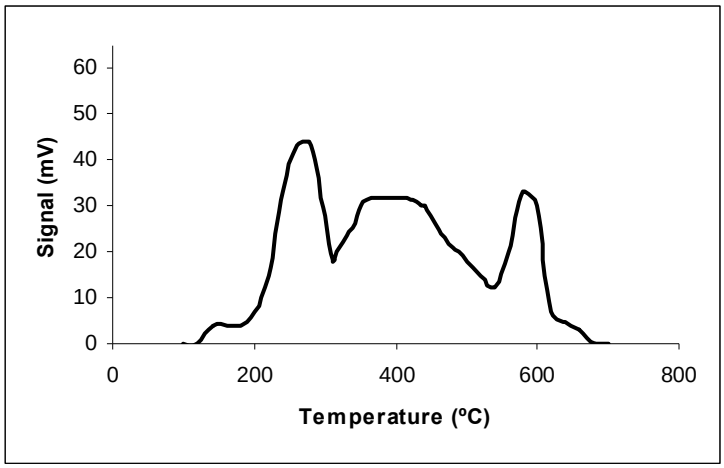

Figure 12. CO_2-TPD of the catalyst NiMgOa.

The peaks that desorb around 280ºC and 600ºC are proportional in intensity (taking into account the magnesia amount) to those of commercial magnesia (Fig.8) whereas the peak around 370ºC can be associated to metallic nickel (Fig.10b), as commented above. Consequently, the interaction Ni-MgO practically does not exist. All these results will be correlated later with the catalytic activity data.

Catalytic activity

Fig. 13 shows the catalytic activity of the three bulk nickel catalysts at room temperature, and at 323 K for the hydrogenation of styrene oxide.

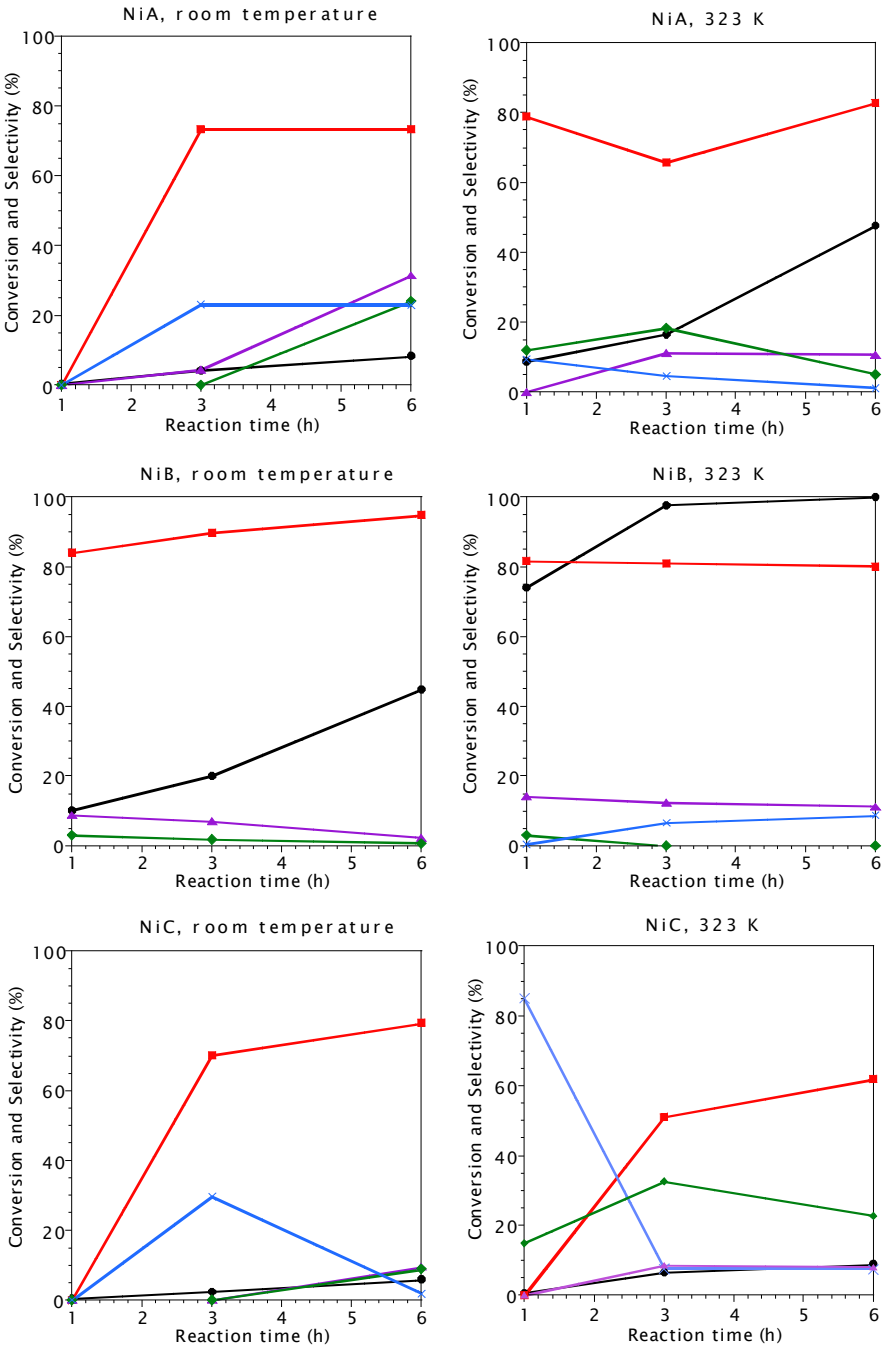

Figure 13. Catalytic activity of the catalyts NiA, NiB, NiC at room temperature and at 323K. Symbols: • Conversion (%), ■ Selectivity to 2-phenylethanol (%), × Selectivity to Condensation Products (%), ▲ Selectivity to Ethylbenzene (%), ◆ Selectivity to Styrene (%).

UNIVERSITAT ROVIRA I VIRGILI
DISEÑO DE CATALIZADORES PARA UNA OBTENCIÓN LIMPIA DE 2-FENILETANOL
Olga Bergadà Miró
ISBN:978-84-691-0355-5/DL:T.2186-2007

These catalysts present low conversion and high selectivity to 2-phenylethanol at room temperature with a maximum of 95 % of selectivity to 2-phenylethanol for a 45 % of conversion for catalyst NiB at 6 h of reaction. The other products, formed in similar amounts, are ethylbenzene, styrene and condensation products. For all catalysts, an increase of conversion, and selectivity to 2-phenylethanol at expenses of the other reaction products, is observed with the reaction time.

By increasing the reaction temperature (323 K), an important increase of conversion maintaining high selectivity to 2-phenylethanol (around 80%) is obtained for catalysts NiA and NiB, whereas for catalyst NiC the conversion is similar than that observed at room temperature decreasing the selectivity to 2-phenylethanol (≈ 60%). Regarding the other reaction products, a slight increase of ethylbenzene is observed for catalyst NiA and, especially, for NiB (around 10% at 6 h) whereas NiC leads to important amounts of styrene (about 20% at 6 h), and condensation products (particularly at the beginning of reaction, 80% at 1 h). Again, catalyst NiB shows the best catalytic results with selectivity to 2-phenylethanol about 80 % for a total conversion at 6 h of reaction.

The modification of the products distribution observed for the styrene oxide hydrogenation when increasing the reaction temperature should be related to a reaction rate of styrene formation lower than the reaction rate of 2-phenylethanol obtaining. It is important to remark that 1-phenylethanol was not detected for any catalyst under these reaction conditions. This is in agreement with the results reported by other authors when using bulk nickel catalysts of type Raney-Ni [34,36].

NiB is the most active catalyst at the two reaction temperatures tested. This can be due to its higher metallic area (1.7 m^2/g) (Table 3). In contrast, catalysts NiA and NiC, with similar metallic areas (0.5 and 0.6 m^2/g, respectively), show a very different catalytic behaviour. NiC is the less active catalyst with the same low conversion value (10%) at the two reaction temperatures. The detection of higher amounts of styrene than its

corresponding hydrogenated product, ethylbenzene, justifies the low activity of this catalyst. Interestingly, this catalyst showed more defined small octahedral particles than the other bulk nickel catalysts (Fig.7). We think that these octahedral morphologies could favour the formation of more amounts of high-weight condensation products during the first hours of reaction, which can block partially the active centres of the catalyst, decreasing its activity.

Figure 14 shows the results of catalytic activity of one commercial Raney-Ni catalyst at room temperature, and at 323 K for the hydrogenation of styrene oxide. These catalytic studies were made in order to compare them with the results obtained by our catalysts at the same reaction conditions.

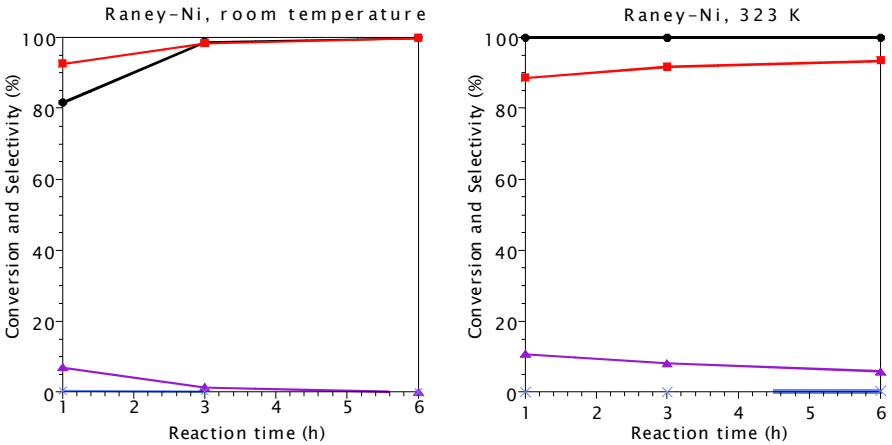

Figure 14. Catalytic activity of commercial Ni-Raney catalyts at room tempertaure and at 323K. Symbols: • Conversion (%), ■ Selectivity to 2-phenylethanol (%), × Selectivity to Condensation Products (%), ▲ Selectivity to Ethylbenzene (%), ◆ Selectivity to Styrene (%).

This commercial Raney-Ni catalyst presents much higher conversion values and higher selectivity to 2-phenylethanol than the prepared bulk nickel catalysts although the differences are higher respect to NiA and NiC than respect to NiB. Also, ethylbenzene was detected in small amounts. This higher conversion can be related to its much higher metallic area (30 m^2/g), whereas the selectivity values should be related to its electronic characteristics that are

UNIVERSITAT ROVIRA I VIRGILI
DISEÑO DE CATALIZADORES PARA UNA OBTENCIÓN LIMPIA DE 2-FENILETANOL
Olga Bergadà Miró
ISBN:978-84-691-0355-5/DL:T.2186-2007

very different respect to the other prepared crystalline bulk nickel catalysts. This allows us to adjudge to the characteristics of the metallic centres an important role in the catalytic behaviour of the studied reaction.

Figure 15 shows the results of catalytic activity of Ni-MgO catalysts at room temperature, and at 323 K for the hydrogenation of styrene oxide.

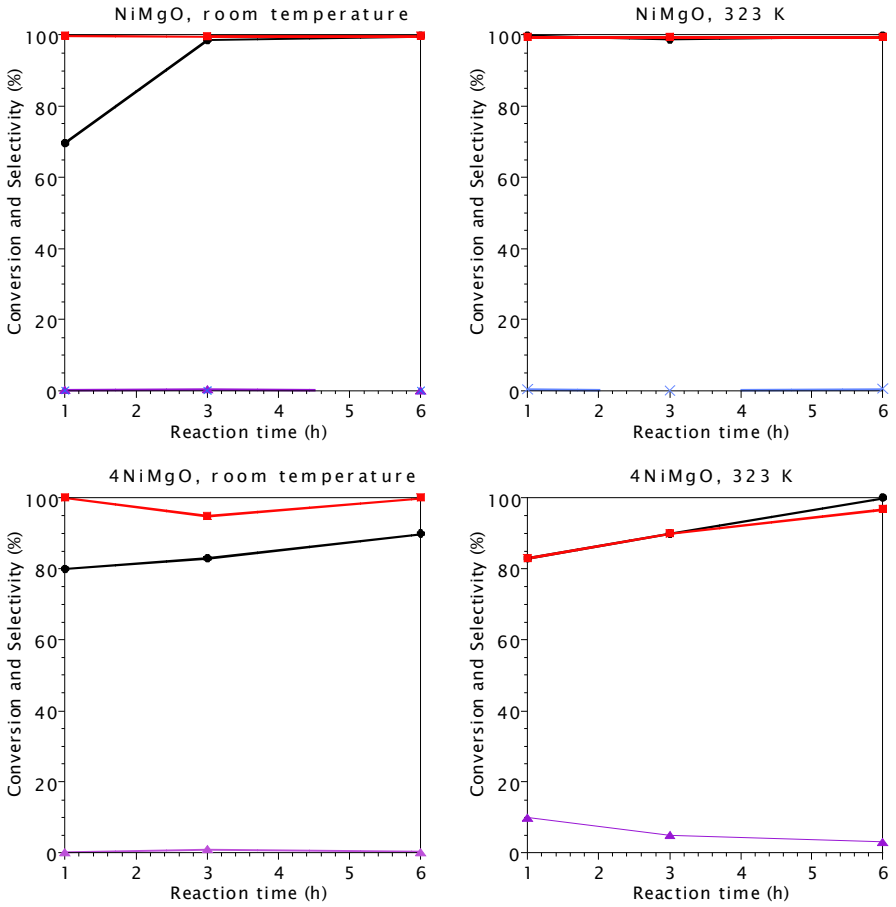

Figure 15. Catalytic activity of the catalysts 4NiMgO and NiMgO at room temperature and at 323K. Symbols: • Conversion (%), ■ Selectivity to 2-phenylethanol (%), × Selectivity to Condensation Products (%), ▲ Selectivity to Ethylbenzene (%), ◆ Selectivity to Styrene (%).

These catalysts present high conversion and high selectivity values to 2-phenylethanol from the first hour of reaction with a maximum of 100% of selectivity to 2-phenylethanol for a total conversion when using catalyst NiMgO at 323 K at any reaction time.

As we can see, the conversion increases when increasing the reaction time, the reaction temperature and the magnesia content. It is important to note that only ethylbenzene in small amounts was observed as by-product, and only for the catalyst with less magnesia content, 4NiMgO. This confirms the importance of the contribution of basicity on the reaction mechanism, and shows magnesia as a good material to obtain the desired basic sites. These results are in agreement with the mechanism proposed by Mitsui et al. for this reaction in basic solution medium (Esquema 7, pg.12) [34]. Additionally, this basicity seems to play a fundamental paper to control the formation of condensation products, which could be responsible for the deactivation of the catalyst, as commented above for catalyst NiC. Thus, both effects of magnesia explain the higher conversion and selectivity to 2-phenylethanol values achieved when using NiMgO catalyst, with higher magnesia content, respect to 4NiMgO.

Another fact to comment is that despite having the same precursor, NiOB, catalyst NiB shows lower conversion, especially at room temperature (Fig.13), than the Ni-MgO catalysts This again confirms the effect of magnesia which avoids the formation of condensation products on the metallic surface giving higher activity to the mixed catalysts.

Figure 16 shows the catalytic activity of the catalysts 4NiMgOr and NiMgOr at room temperature.

UNIVERSITAT ROVIRA I VIRGILI
DISEÑO DE CATALIZADORES PARA UNA OBTENCIÓN LIMPIA DE 2-FENILETANOL
Olga Bergadà Miró
ISBN:978-84-691-0355-5/DL:T.2186-2007

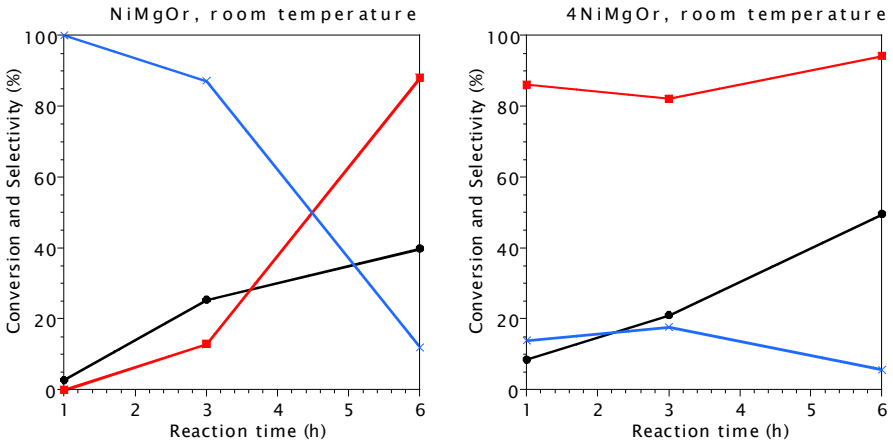

Figure 16. Catalytic activity of the catalysts 4NiMgOr and NiMgOr at room temperature. Symbols: • Conversion (%), ■ Selectivity to 2-phenylethanol (%), × Selectivity to Condensation Products (%), ▲ Selectivity to Ethylbenzene (%), ◆ Selectivity to Styrene (%).

By using NiMgOr and 4NiMgOr catalysts, much lower conversion and lower selectivity to 2-phenylethanol values at expenses of higher amounts of condensation products were observed.

Finally, catalysts NiMgOa and 4NiMgOa show low conversion and very low or null selectivity to 2-phenylethanol (Figure 17).

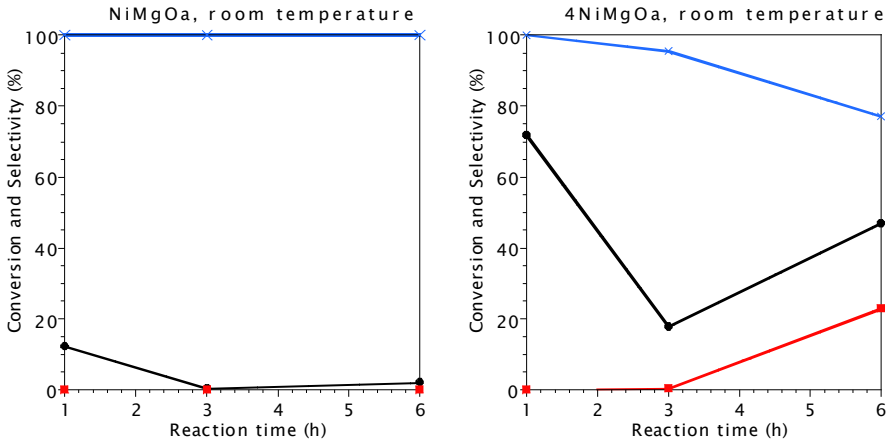

Figure 17. Catalytic activity of the catalysts 4NiMgOr and NiMgOr at room temperature. Symbols: Symbols: • Conversion (%), ■ Selectivity to 2-phenylethanol (%), × Selectivity to Condensation Products (%), ▲ Selectivity to Ethylbenzene (%), ◆ Selectivity to Styrene (%).

We detected very high amounts of condensation products in these catalysts (77 % for 4NiMgOa and 100 % for NiMgO).

The metallic area of these catalysts cannot explain these catalytic results, since the highest metallic area (1.2 m^2/g) (Table 3) corresponds to the catalyst 4NiMgOa with low conversion and very low selectivity to 2-phenylethanol. Interestingly, the catalytic behavior of these catalysts with magnesia could be related to the different CO_2-TPD profiles observed for these catalysts. Thus, the catalyst with higher MgO content (NiMgO), whose CO_2-TPD showed metallic nickel partially covering the weakest basic sites of magnesia (Fig.10a) is more active and selective to 2-phenylethanol than the rest of catalysts. On the other hand, the CO_2-TPDs of catalysts NiMgOr and NiMgOa showed an important amount of available basic sites that favour the formation of higher amounts of condensation products, which are responsible for the catalyst deactivation [13]. In these Ni-MgOr and Ni-MgOa systems the interaction between metallic and basic particles are very low or null. Therefore, we can conclude that the metallic nickel under the influence of the weakest basic sites of commercial magnesia should be related to the selective formation of 2-phenylethanol. This minimizes the formation of other reaction products such as ethylbenzene or condensation products, which were not detected in these catalysts.

Interestingly, the catalyst with higher magnesia content, NiMgO, shows similar conversion values but higher selectivity to 2-phenylethanol (Fig. 15) than the Raney-Ni catalyst (Fig.14). This reveals, again, the effect of magnesia which favours the selective formation of 2-phenylethanol.

The catalytic lifetime of the best catalyst (NiMgO) was also tested (Fig.18). After reusing the catalyst once, the same conversion and selectivity values were obtained. When the catalyst is used again we observe a slight conversion decrease from 100% to 83%, whereas the selectivity to 2-phenylethanol remains around 95 %. These catalytic activity values are maintained when the catalyst is reused three more times. These slight variations could be explained by the formation of small amounts of

UNIVERSITAT ROVIRA I VIRGILI
DISEÑO DE CATALIZADORES PARA UNA OBTENCIÓN LIMPIA DE 2-FENILETANOL
Olga Bergadà Miró
ISBN:978-84-691-0355-5/DL:T.2186-2007

condensation products, which block some metallic sites. Therefore, there is a clear influence of basicity in the catalytic behaviour of these Ni-MgO systems.

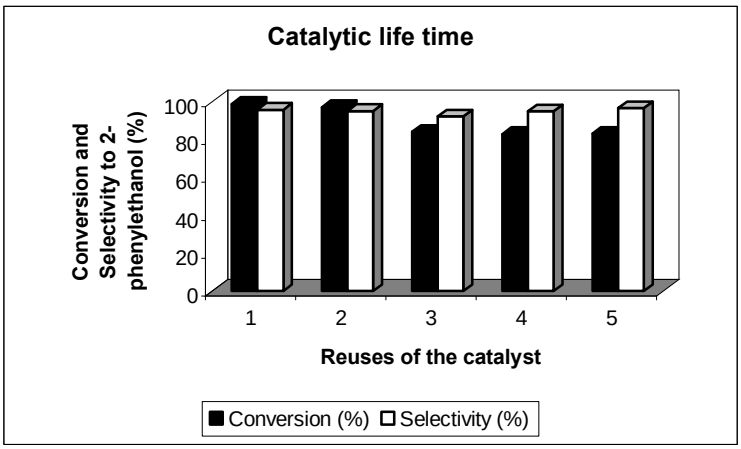

Figure 18. Catalytic life time of the best catalyst NiMgO.

4.1.4 Conclusions

The bulk nickel catalysts prepared present high selectivity to 2-phenylethanol (60-95%) despite their different conversion values. These catalysts give to the formation of condensation products which block the active centres of the catalyst, decreasing its activity. This behaviour appears more marked for catalyst NiC (the less active) which, interestingly, is the catalyst that showed more homogeneous and defined octahedral particles. When increasing the temperature of reaction, an increase of the conversion as well a certain decrease of the selectivity to 2-phenylethanol is observed at expenses of styrene and ethylbenzene formation. The most active of the bulk nickel catalysts prepared is catalyst NiB. This can be related to its higher metallic area.

On the other hand, the basic sites available in the Ni-MgO catalysts determine the distribution of the reaction products for the hydrogenation of styrene oxide. Catalysts with commercial MgO (NiMgO and 4NiMgO) present conversion and selectivity to 2-phenylethanol values that increase when the content of magnesia increases arriving to 100% for catalyst NiMgO at the two temperatures of reaction tested. The CO_2-TPD profile of the best catalyst, NiMgO, showed the disappearance of the peak corresponding to the weaker basic sites of commercial magnesia. This means that the metallic nickel, obtained after reduction, cover these basic sites and, therefore, there is some influence between the nickel particles and the basic sites, which become less available. The existence of a certain interaction between the nickel and the weakest basic sites of magnesia in these Ni-MgO catalysts favour the quickly formation of 2-phenylethanol, and consequently, minimizes other side reactions like the formation of condensation products. This explains the higher conversion and selectivity to 2-phenylethanol values of these Ni-MgO catalysts despite having lower metallic area than NiB and Raney-Ni catalysts.

In contrast, the CO_2-TPD profiles obtained for catalysts NiMgOr and NiMgOa showed that they have higher amounts of basic sites available. This can explain the higher amounts of condensation products, detected for catalysts NiMgOr, 4NiMgOr, NiMgOa and 4NiMgOa, which are responsible for their lower activity.

The catalyst prepared with the highest amount of commercial magnesia (NiMgO) maintains high conversion and selectivity to 2-phenylethanol values after reusing several times.

UNIVERSITAT ROVIRA I VIRGILI
DISEÑO DE CATALIZADORES PARA UNA OBTENCIÓN LIMPIA DE 2-FENILETANOL
Olga Bergadà Miró
ISBN:978-84-691-0355-5/DL:T.2186-2007

4.2 Catalytic systems based on Hydrotalcite-like compounds

4.2.1 Introduction

Hydrotalcite-like compounds, a class of layered materials having the general formula $[M(II)_{1-x}M(III)_x(OH)_2][A_{x/n}^{n-}]mH_2O$, have been receiving increasing attention in the last years owing to their potential applications as basic catalysts, supports, ion-exchangers and precursors for composite materials [77-79]. Structurally, layered double hydroxides (LDHs) have brucite-like ($Mg(OH)_2$) sheets where isomorphous substitution of Mg^{2+} by a trivalent cation, like Al^{3+}, occurs (Fig. 19). The resulting positive charge excess of the layered network is compensated by anions, which occupy the interlayer space along with water molecules. Their basicity is mainly related to the amount and nature of divalent cations present.

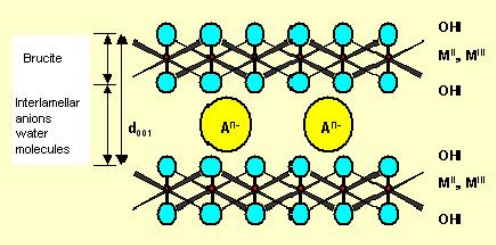

Figure 19. Hidrotalcite structure.

Controlled thermal decomposition of hydrotalcites gives to high-area mixed oxides that have numerous catalytic applications such as the removal of SO_x and NO_x, aldol condensations, phenol alkylations, epoxidation of olefines, and partial oxidation, hydrodehalogenation or hydrogenation reactions [80-89]. The acidic-basic properties of calcined hydrotalcites can be tailored by changing the calcination temperature, the nature and amount of structural cations and compensating anions, as well as, the method of synthesis of the LDHs [77,90]. Besides, these mixed oxides show a memory effect, a property by which they can recover the original lamellar structure if they come in contact with water vapour or are immersed in liquid water. These

rehydrated materials have been applied to a number of base-catalyzed reactions on account of their Brønsted basic character [81,91,92].

Unfortunately, hydrotalcites are not often found in nature so they have to be synthesized. Hydrotalcites are conventionally prepared by coprecipitation, wherein metal nitrates and precipitants are added slowly and simultaneously at a fixed pH under stirring. The main disadvantage of this method is the time required to crystallize the hydrotalcite. Thus, the precipitated gel has to be aged for a long time (about one day) [93,94]. New synthetic routes have been explored, for instance the sol-gel method, but expensive reactants are required and the resulting solid is not fully crystalline [95].

Microwave irradiation has been widely used for the synthesis of inorganic solids and in organic synthetic reactions [96,97]. From middle of 90s, the formation of well-crystallized and pure hydrotalcite-like phases, when aging the coprecipitated gels under microwaves, have been reported with a considerably decrease of the aging time. On the whole, these hydrotalcites aged under microwaves present smaller particles sizes and higher surface areas than conventional samples [98-102]. The most part of studies published concerns the influence of the microwave irradiation power on the aging of binary hydrotalcite gels [103-105], basically Mg/Al, and the study of the basic properties of the resulting mixed oxides [104]. Recently, the effect of microwave power on Zn/Mg/Al gels and the influence of the irradiation temperature of aged Mg/Al gels on the surface properties of calcined samples have been reported [106,107].

Interestingly, Tichit et al. reported the presence of surface-defective sites with an increase of both basic and acid sites in the resulting Mg/Al mixed oxides when the hydrotalcite was aged by microwave irradiation [108]. Also, a decrease of aluminium in the hydrotalcite structure accompanied by the formation of hydroxylated aluminium species in the extraframework has been detected in some cases. This could be related to some erosion of the hydrotalcite layers because of the microwaves interaction [108-110].

UNIVERSITAT ROVIRA I VIRGILI
DISEÑO DE CATALIZADORES PARA UNA OBTENCIÓN LIMPIA DE 2-FENILETANOL
Olga Bergadà Miró
ISBN:978-84-691-0355-5/DL:T.2186-2007

The basicity of the hydrotalcites and the mixed oxides obtained after their calcination can be studied by temperature-programmed desorption (TPD) using an acid probe molecule, such as CO_2. This technique also can allow us to study the surface modifications associated to the acid-basic properties of these materials.

Firstly, in this chapter, we present a systematic study on several hydrotalcites of Ni/Mg/Al prepared from coprecipitated gels with the same composition using a laboratory microwave oven, equipped with a temperature controller, to age the gel at various temperatures and times in order to study the influence of treatment conditions on the basic and surface properties of the resulting hydrotalcites and their calcination compounds. Besides, we synthesized these Ni/Mg/Al hydrotalcites aged by the traditional refluxing method and by autoclaving for comparison. All samples were characterized by a wide number of techniques.

Taking into account the good results found by using basic Ni-MgO catalysts, as commented in the previous chapter, we believe that Ni/Mg/Al hydrotalcites can be good candidates to be used as catalytic precursors for the hydrogenation of styrene oxide in order to obtain selectively 2-phenylethanol since, after calcination-reduction, they can lead to well-dispersed metallic nickel interacting with basic sites. Hydrotalcites were prepared using low amounts of Mg and Al in order to avoid high basicity that could be responsible for undesirable reactions [36]. Several catalysts based on hydrotalcite-like compounds have been tested in the hydrogenation of styrene oxide in the liquid phase in order to study the influence of the hydrotalcites aging step on their surface properties and, consequently, on the catalytic behaviour of the resulting catalysts.

4.2.2 Experimental

Catalysts preparation

The starting gel was synthesized by the traditional coprecipitation method at room temperature at constant pH (pH = 8 ± 0.1), using an aqueous solution containing in appropriate amounts $Ni(NO_3)_2 6H_2O$, $Mg(NO_3)_2 6H_2O$ and $Al(NO_3)_3 9H_2O$, and a 1M NaOH titrating solution which were simultaneously added to an aqueous solution of $Na_2CO_3 10H_2O$ 0.05M. The ratio M^{2+}/Al^{3+} was 4:1 and the ratio Ni^{2+}/Mg^{2+} was 6:1. Dropwise addition was performed under vigorous magnetic stirring. After complete precipitation, the gel was aged at different conditions resulting in 27 samples to be compared.

One sample was obtained by refluxing the gel under stirring at 343 K for 1080 min (R_{1080}). Four samples were obtained by refluxing the gel under microwave irradiation at 343 K for 60, 120, 240 and 480 min, respectively (RMW_{60}, RMW_{120}, RMW_{240}, RMW_{480}). Another four samples were aged in an autoclave in an oven at 403 and 423 K for 120 and 360 min, respectively ($403A_{120}$, $403A_{360}$, $423A_{120}$, $423A_{360}$). The last series of samples were aged in an autoclave into a microwave oven (Milestone ETHOS-TOUCH CONTROL) at 403 K, 423 K and 453 K for 1, 5, 15, 30, 60 and 120 min for each temperature ($403MW_1$, $403MW_5$, $403MW_{15}$, $403MW_{30}$, $403MW_{60}$, $403MW_{120}$, $423MW_1$, $423MW_5$, $423MW_{15}$, $423MW_{30}$, $423MW_{60}$, $423MW_{120}$, $453MW_1$, $453MW_5$, $453MW_{15}$, $453MW_{30}$, $453MW_{60}$, $453MW_{120}$). Finally, all samples were filtered and washed several times with deionised water and the solids were dried in an oven at 393 K overnight.

Five of these samples ($403MW_{15}$, $453MW_{120}$, RMW_{120}, R_{1080} and $403A_{360}$) were calcined flowing nitrogen through the sample (2 ml/s) at 623 K for 3 h to obtain the samples named as $R_{1080}C$, $403A_{360}C$, $RMW_{120}C$, $403MW_{15}C$ and $453MW_{120}C$. These catalytic precursors were reduced flowing hydrogen through the sample (2 ml/s) at 623 K for 6 h to obtain the corresponding catalysts named as $R_{1080}R$, $403A_{360}R$, $RMW_{120}R$, $403MW_{15}R$ and $453MW_{120}R$

UNIVERSITAT ROVIRA I VIRGILI
DISEÑO DE CATALIZADORES PARA UNA OBTENCIÓN LIMPIA DE 2-FENILETANOL
Olga Bergadà Miró
ISBN:978-84-691-0355-5/DL:T.2186-2007

Air-free sampling

The catalysts were always handled under air-free conditions after the reduction step. The catalysts were transferred in degassed cyclohexane and under a hydrogen atmosphere at room temperature. The cyclohexane surface-impregnated samples were further isolated from the air with sticky tape for XRD monitoring, where a glove box was used for mounting.

Characterization of the samples

The catalytic precursors and the catalysts were characterized by Infrared Spectroscopy, X-Ray Diffraction (XRD), Nitrogen physisorption, Scanning electron microscopy (SEM), Transmission electron microscopy (TEM), Temperature-programmed desorption-mass spectrometry experiments (CO_2-TPD and H_2-TPD), Atomic absorption, Thermogravimetric analyses (TGA) and Hydrogen Chemisorption. The experimental conditions used have been indicated in the Experimental Section (3.2).

Catalytic activity determination

The catalytic hydrogenation of styrene oxide was made in the liquid phase, using for all tests 0.5 g of active phase, 20 mL of absolute ethanol (Panreac, 99.5%) and 4 mmol of styrene oxide (Aldrich, 97%) with a hydrogen flow of 2 ml/s and agitation of 700 rpm. The reaction was performed at room temperature. Sample was taken each 15 minutes. The reaction products were analyzed by gas chromatography, using a chromatograph Shimadzu GC-2010 with 30 m of capillary column "DB-1" and a FID detector. They were quantified by adding an internal standard and by using a calibrated line. We also tested the catalytic lifetime of these catalysts by reusing them ten times at the same reaction conditions.

4.2.3 Results and discussion

Characterization of the hydrotalcites

- **X-Ray diffraction (XRD)**

Figs. 20-22 show the XRD patterns obtained for all samples whereas tables 4 and 5 exhibit the FWHM and cell parameters values.

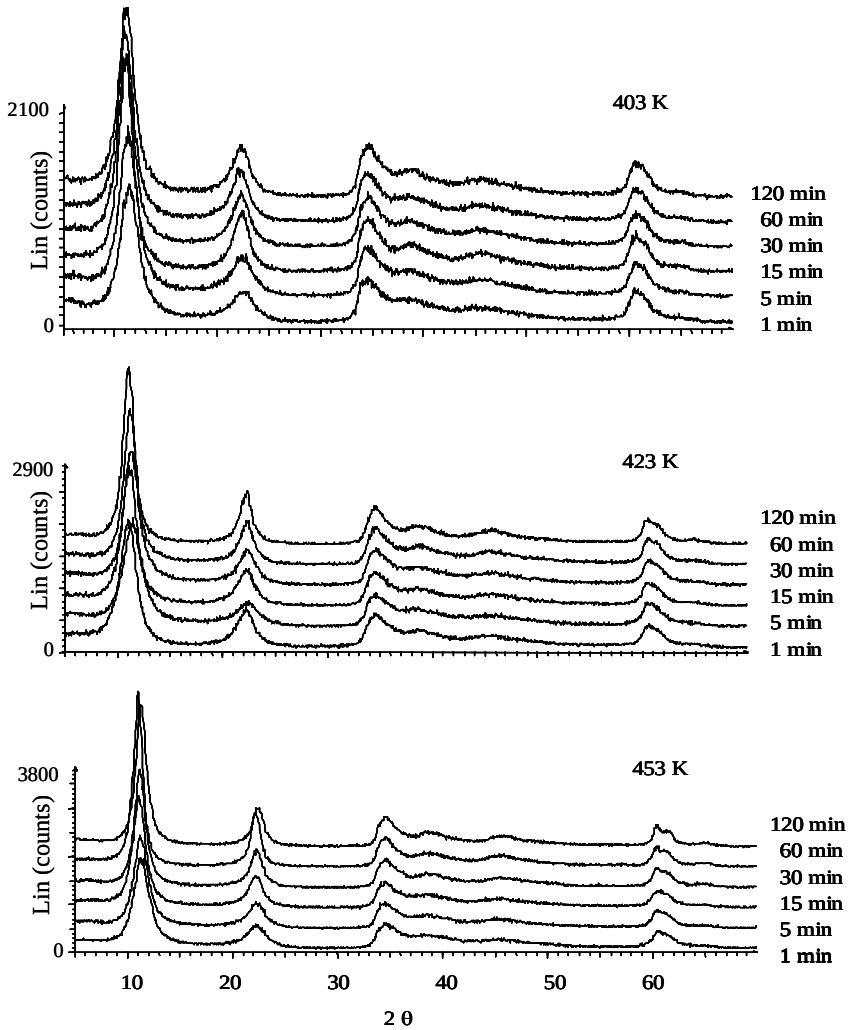

Figure 20. XRD patterns of the hydrotalcites aged in an autoclave under microwaves.

UNIVERSITAT ROVIRA I VIRGILI
DISEÑO DE CATALIZADORES PARA UNA OBTENCIÓN LIMPIA DE 2-FENILETANOL
Olga Bergadà Miró
ISBN:978-84-691-0355-5/DL:T.2186-2007

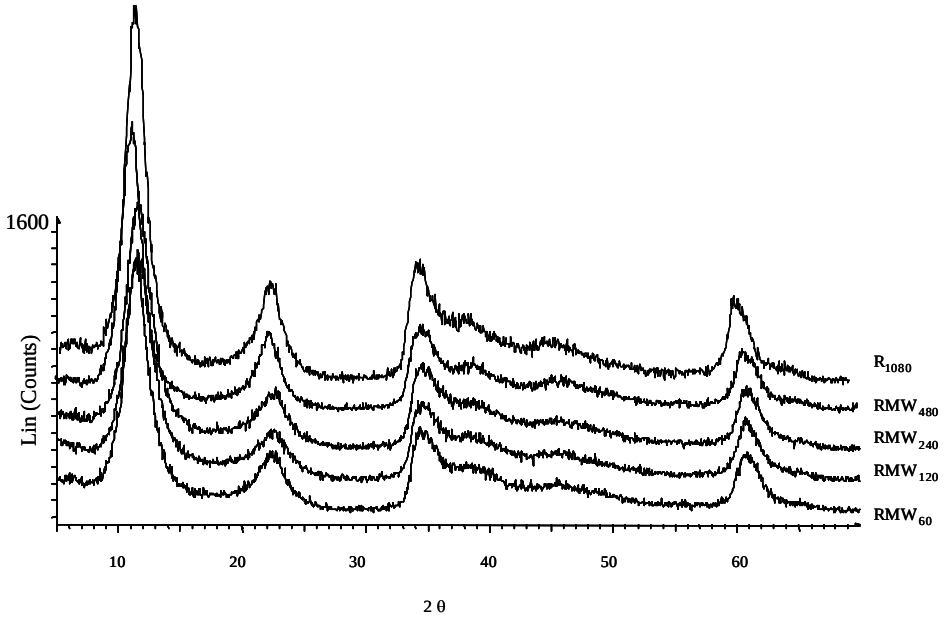

Figure 21. XRD patterns of the hydrotalcites aged by conventional refluxing and by refluxing under microwave irradiation.

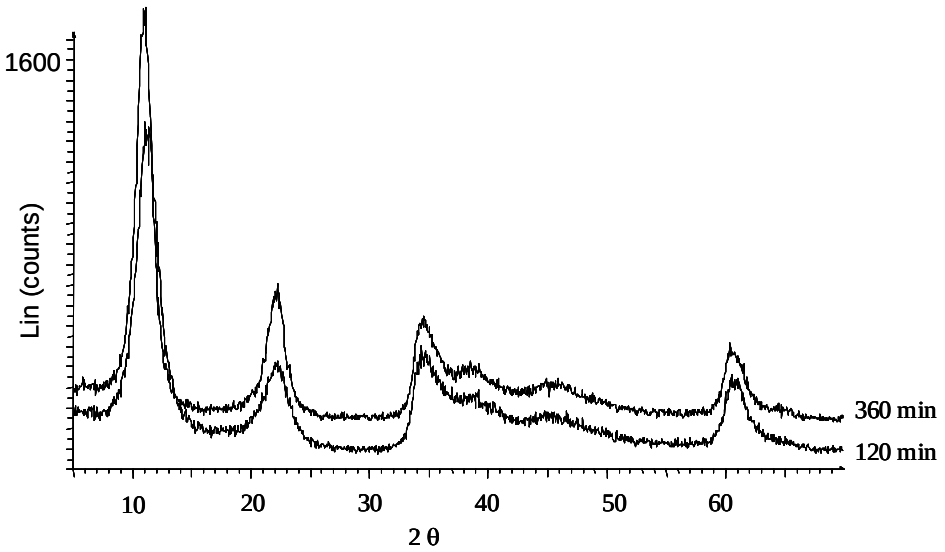

Figure 22. XRD patterns of the hydrotalcites aged by heating in a conventional oven at 403 K.

Table 4. Characterization results obtained by XRD and nitrogen physisorption for the samples aged under microwave irradiation.

	FWHM[a] (degrees)	c (nm)	a (nm)	Surface Area (m^2/g)
403MW$_1$	2.06	2.336	0.306	32.0
403MW$_5$	2.00	2.362	0.305	20.3
403MW$_{15}$	1.82	2.398	0.305	12.6
403MW$_{30}$	1.80	2.399	0.305	3.7
403MW$_{60}$	1.77	2.408	0.306	4.4
403MW$_{120}$	1.76	2.383	0.306	2.9
423MW$_1$	2.05	2.415	0.306	26.9
423MW$_5$	1.84	2.339	0.306	14.5
423MW$_{15}$	1.66	2.398	0.306	11.8
423MW$_{30}$	1.63	2.361	0.306	2.6
423MW$_{60}$	1.43	2.383	0.306	< 2.5
423MW$_{120}$	1.23	2.411	0.306	< 2.5
453MW$_1$	1.74	2.367	0.306	< 2.5
453MW$_5$	1.56	2.376	0.306	< 2.5
453MW$_{15}$	1.38	2.401	0.306	< 2.5
453MW$_{30}$	1.23	2.389	0.306	8.0
453MW$_{60}$	1.00	2.415	0.306	11.9
453MW$_{120}$	0.94	2.407	0.306	87.2
RMW$_{60}$	2.05	2.301	0.305	2.5
RMW$_{120}$	2.04	2.345	0.305	3.3
RMW$_{240}$	2.02	2.302	0.305	3.4
RMW$_{480}$	1.80	2.370	0.305	3.2

[a] FWHM values have been measured for peak (003).

Table 5. Characterization results obtained by XRD and nitrogen physisorption for the samples aged by conventional methods.

	FWHM[a] (degrees)	c (nm)	a (nm)	surface area (m^2/g)
403A$_{120}$	2.01	2.379	0.305	< 2.5
403A$_{360}$	1.79	2.333	0.306	< 2.5
423A$_{120}$	1.76	2.381	0.306	2.9
423A$_{360}$	1.45	2.386	0.306	< 2.5
R$_{1080}$	1.87	2.359	0.306	32.3

[a] FWHM values have been measured for peak (003).

UNIVERSITAT ROVIRA I VIRGILI
DISEÑO DE CATALIZADORES PARA UNA OBTENCIÓN LIMPIA DE 2-FENILETANOL
Olga Bergadà Miró
ISBN:978-84-691-0355-5/DL:T.2186-2007

Hydrotalcite-like compounds have characteristic XRD patterns with sharp and intense peaks for the (003), (006), (110) and (113) planes, as well as broad symmetric peaks for the (009), (015) and (016) planes. The full width at half maximum (FWHM) of the basal reflection plane (003) is usually taken to evaluate their cristallinity in the stacking direction.

In the starting precipitated gel, without aging, as well as in the 27 samples aged at different conditions (Figs. 20-22) only one phase, corresponding to hydrotalcite, was detected. On the whole, the crystallinity of the hydrotalcites is low although they show different crystallinity degrees. Once measured the FWHM values, we can see that the starting precipitated gel without aging has higher FWHM value (2.06), and therefore, lower crystallinity than the samples aged by any method (Tables 4 and 5).

For the hydrotalcites aged in an autoclave by microwaves, the FWHM values decrease when increasing the aging time and the aging temperature (Table 4) indicating an increase of the crystallinity. Therefore, both factors, higher temperatures and longer times of aging, favour crystallization in the stacking direction. Thus, the hydrotalcite aged at 453 K for 120 min is the most crystalline. The better resolution of the peaks at higher 2θ values, specifically those which correspond to the (110) and (113) planes, also confirms a higher interlayer ordering in this sample (Fig. 20). For the hydrotalcites aged by refluxing under microwaves, the FWHM values also decrease when increasing the aging time but less significantly than for the samples aged by autoclaving under microwaves (Table 4). It is well known that the crystallization of hydrotalcites is a consequence of the growing of the seeds formed during the coprecipitation process [110]. Therefore, the variation of the FWHM values with time allows us to interpret when the seeds formed during coprecipitation begin growing favouring the crystallization. Taking as a reference the FWHM value of the coprecipitated gel without aging (2.06), for the hydrotalcites aged in an autoclave by microwaves at 403 K, 15 min are necessary to detect a significant growing of the seeds whereas for the hydrotalcites aged at 423 K and at 453 K only 5 min and 1 min are needed,

respectively (Table 4). In contrast, the hydrotalcites aged by refluxing under microwaves need more than 240 min to obtain a noticeable crystallization of the seeds (Table 4). Furthermore, these hydrotalcites are less crystalline than those obtained by autoclaving under microwaves.

By comparing the hydrotalcites prepared by refluxing under microwaves and by conventional method (Fig. 21), we observe that sample R_{1080}, prepared by refluxing without microwaves at 343 K for 1080 min, has similar crystallinity in the stacking direction (FWHM = 1.87) (Table 5) than the hydrotalcite $RMW_{480,}$ aged by refluxing under microwaves at the same temperature for 480 min (FWHM = 1.84) (Table 4). Therefore, we obtained hydrotalcites with higher crystallinity in the half of time when using microwaves.

This effect was also observed by comparing the hydrotalcites aged in an autoclave with and without microwaves (Figs. 20 and 22). The crystallinity of the hydrotalcites aged in a conventional autoclave at 403 and 423 K for 360 min and 120 min, respectively (samples $403A_{360}$ and $423A_{120}$) is similar to that of the hydrotalcites obtained in an autoclave by microwave irradiation at the same temperatures at 30 min and less than 15 min, respectively (samples $403MW_{30}$ and $423MW_{15}$) (Tables 4 and 5). Besides, the seeds begin growing approximately twelve times faster in the hydrotalcites aged in an autoclave by microwaves at 403 K and at 423 K than those prepared in a conventional oven.

The cell parameters (*a* and *c*), calculated from the (110) and (003) interplanar distances, respectively, were determined in order to obtain information about modifications in the sheets and in their stacking for all the hydrotalcites prepared (Tables 4 and 5). The cell parameter *a*, which is mainly related to the cation composition, practically does not change (*a*= 0.305-0.306). Taking into account that nickel is the main component of these hydrotalcites, the very low differences observed in the *a* values could indicate that the nickel composition of the samples does not practically vary. For the cell parameter *c*, which is proportional to the interplanar distance, any defined

UNIVERSITAT ROVIRA I VIRGILI
DISEÑO DE CATALIZADORES PARA UNA OBTENCIÓN LIMPIA DE 2-FENILETANOL
Olga Bergadà Miró
ISBN:978-84-691-0355-5/DL:T.2186-2007

tendency cannot be observed. The variations observed could be due to the different distribution of the species in the interlamellar space.

- **Nitrogen physisorption**

The specific surface areas measured for all the hydrotalcites aged with and without microwaves are summarized in tables 4 and 5, respectively.

The BET area of the coprecipitated gel without aging is 38.6 m^2/g. Having in mind this value, the surface area decreases when increasing the microwave irradiation time for the samples aged in an autoclave at 403 K and 423 K. This can be related to the increase of the crystallinity observed by XRD (Fig. 20, Table 4). On the other hand, the hydrotalcites aged in an autoclave under microwaves at 453 K have low surface areas the first 15 min (< 2.5 m^2/g). However, after this time, a considerably increase of the surface area was observed (87.2 m^2/g at 120 min). These results are very surprising since XRD results showed an increase of the crystallinity with the increase of the aging time, as expected (Fig. 20, Table 4). This area increase suggests the existence of some microwave effect on the surface of the sample that has been already commented by other authors [108].

The samples aged in an autoclave without microwaves at 403 K and 423 K ($403A_{120}$, $403A_{360}$, $423A_{120}$, $423A_{360}$) have not practically surface areas (Table 5).

Respect to the hydrotalcites aged by refluxing, the sample prepared by conventional refluxing (R_{1080}) has higher surface area than those refluxed under microwaves (Tables 4 and 5). Taking into account that similar FWHM values were obtained for all the refluxed samples, the higher surface area of sample R_{1080} could be explained by the remaining mesoporosity which was also observed in the starting coprecipitated gel, as commented below.

Figs. 23 and 24 show the N_2 adsorption-desorption isotherms and the pore size distribution graphics of some representative hydrotalcites. Although all the hydrotalcites prepared show a nitrogen adsorption isotherm of type IV,

the hysteresis loops differ depending on the aging conditions. However, we can establish three main groups of samples.

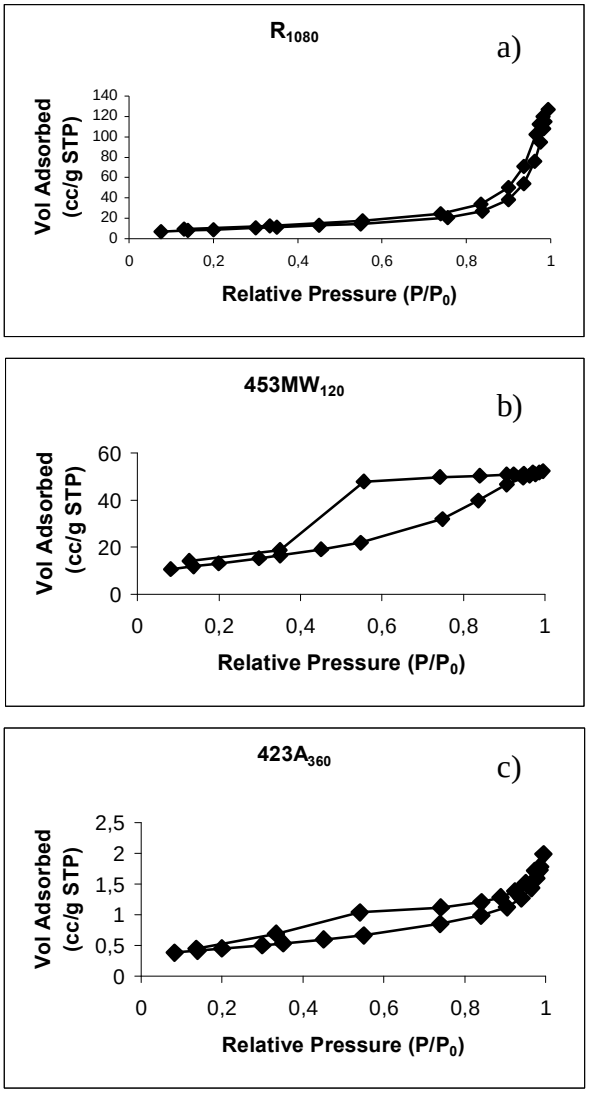

Figure 23. N_2asorption / desorption isotherms at 77 K for the samples: a) R_{1080}, b) $453MW_{120}$ and c) $423A_{360}$.

UNIVERSITAT ROVIRA I VIRGILI
DISEÑO DE CATALIZADORES PARA UNA OBTENCIÓN LIMPIA DE 2-FENILETANOL
Olga Bergadà Miró
ISBN:978-84-691-0355-5/DL:T.2186-2007

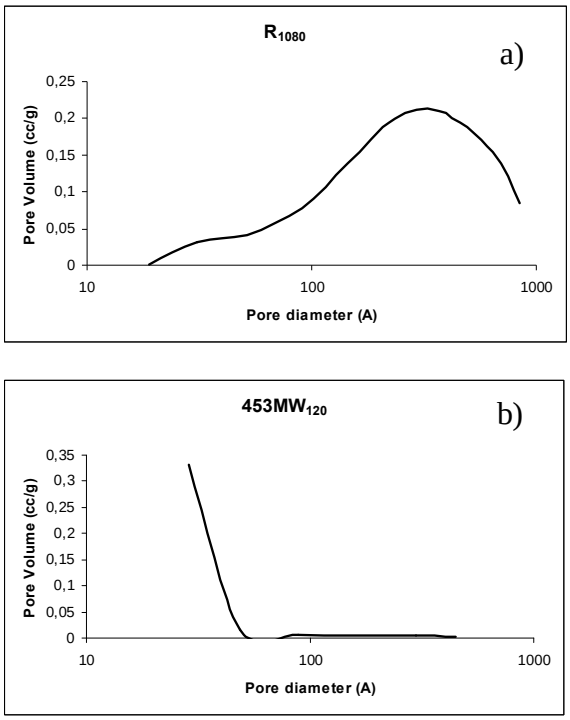

Figure 24. Pore size distribution from the N_2 desorption isotherms at 77 K of the samples: a) R_{1080} and b) $453MW_{120}$.

Figure 23a depicts the nitrogen adsorption-desorption isotherm for the sample aged by conventional refluxing (R_{1080}). This isotherm is very similar to those of the samples aged by refluxing under microwave irradiation (RMW_{60}, RMW_{120}, RMW_{240}, RMW_{480}) and those of the samples aged in an autoclave under microwaves at 403 K and 423 K ($403MW_1$, $403MW_5$, $403MW_{15}$, $403MW_{30}$, $403MW_{60}$, $403MW_{120}$, $423MW_1$, $423MW_5$, $423MW_{15}$, $423MW_{30}$, $423MW_{60}$, $423MW_{120}$). The adsorption and desorption ways are quite similar for these mesoporous samples. The pore size distribution graphic for sample R_{1080} (Fig. 24a) shows a main peak around 350 Å that also appears for all the samples of this group. This is in agreement with the typical mesoporosity described for the hydrotalcites obtained by conventional refluxing [79]. However, this porosity decreases with the time of aging for these microwaved samples as confirmed by the surface area decrease observed (Tables 4 and 5).

On the other hand, the samples aged at 453 K by microwaves from more than 15 min constitute the second group of samples. The N_2 isotherm for the hydrotalcite aged by microwaves at 453 K for 120 min (Fig. 23b) is very similar to those of the samples prepared at this temperature for 30 and 60 min ($453MW_{30}$, $453MW_{60}$). In this case, the adsorption and desorption ways are quite different. This could be associated to an increase of the mesoporosity of low pore diameter observed in the pore size distribution graphics where only one peak under 30 Å appears for these samples (Fig. 24b). This is confirmed by the higher surface area (Table 4) and the increase of pore volume observed especially at longer times of aging (Fig. 24b). These new surface properties could be related to some disaggregations of the hydrotalcite layers due to some local overheating during microwave treatment at the conditions used for these samples. This gives to the formation of surface-defective sites which are responsible for the new porosity and the area increase although we cannot completely discard the presence of small amounts of insoluble amorphous species that can also contribute to the area increase.

The samples aged in an oven at 403 K and 423 K for 120 min and 360 min ($403A_{120}$, $403A_{360}$, $423A_{120}$, $423A_{360}$) together with the samples aged under microwave irradiation at 453 K for 1, 5 and 15 min ($453MW_1$, $453MW_5$, $453MW_{15}$) form the third group of samples. They show a nitrogen adsorption-desorption isotherm similar to that of the sample $453MW_{120}$ (Fig. 23b) but in this case, the difference between the adsorption and desorption ways is lower (Fig. 23c) than for the sample $453MW_{120}$. The pore size distribution graphics of this group of samples exhibit in general two peaks, one around 350 Å and another around 30 Å. The contribution of the peak at 30 Å increases with the time of aging. The low porous volumes and the low surface area values obtained for these samples (Tables 4 and 5) mean that the initial mesoporosity decreases but practically no additional porosity appears.

UNIVERSITAT ROVIRA I VIRGILI
DISEÑO DE CATALIZADORES PARA UNA OBTENCIÓN LIMPIA DE 2-FENILETANOL
Olga Bergadà Miró
ISBN:978-84-691-0355-5/DL:T.2186-2007

➢ Elemental chemical analysis

In this study, the atomic absorption of 9 representative samples was performed in order to determine the chemical formulae, and mainly to detect the possible material loss as a consequence of the microwave treatment. The carbonate content has been obtained from decomposition studies using a calibrated detector whereas the amount of nitrate has been calculated as the difference between the total anions content, determined from the M(II)/M(III) ratio, and the carbonate values. The interlayer water was calculated from TG curves. The results are shown in table 6.

Table 6. Chemical analysis for the most representative samples.

Sample	Ni/Al	Mg/Al	Ni/Mg	Chemical formula[a]
R_{1080}	3.40	0.60	5.67	$[Ni_{0.68}Mg_{0.12}Al_{0.20}(OH)_2][(CO_3^{2-})_{0.08}(NO_3^-)_{0.04}]1.10\ H_2O$
RMW_{480}	3.89	0.67	5.83	$[Ni_{0.70}Mg_{0.12}Al_{0.18}(OH)_2][(CO_3^{2-})_{0.08}(NO_3^-)_{0.02}]0.84\ H_2O$
$403MW_{120}$	3.89	0.67	5.83	$[Ni_{0.70}Mg_{0.12}Al_{0.18}(OH)_2][(CO_3^{2-})_{0.08}(NO_3^-)_{0.02}]0.87\ H_2O$
$423MW_{120}$	4.18	0.71	5.91	$[Ni_{0.71}Mg_{0.12}Al_{0.17}(OH)_2][(CO_3^{2-})_{0.06}(NO_3^-)_{0.05}]0.88\ H_2O$
$453MW_{5}$	4.18	0.71	5.91	$[Ni_{0.71}Mg_{0.12}Al_{0.17}(OH)_2][(CO_3^{2-})_{0.07}(NO_3^-)_{0.03}]0.90\ H_2O$
$453MW_{30}$	4.50	0.75	6.00	$[Ni_{0.72}Mg_{0.12}Al_{0.16}(OH)_2][(CO_3^{2-})_{0.06}(NO_3^-)_{0.04}]0.81\ H_2O$
$453MW_{120}$	6.90	1.18	5.84	$[Ni_{0.76}Mg_{0.13}Al_{0.11}(OH)_2][(CO_3^{2-})_{0.04}(NO_3^-)_{0.03}]0.74\ H_2O$
$403A_{360}$	3.63	0.63	5.75	$[Ni_{0.69}Mg_{0.12}Al_{0.19}(OH)_2][(CO_3^{2-})_{0.06}(NO_3^-)_{0.07}]0.86\ H_2O$
$423A_{360}$	3.63	0.63	5.75	$[Ni_{0.69}Mg_{0.12}Al_{0.19}(OH)_2][(CO_3^{2-})_{0.06}(NO_3^-)_{0.07}]0.86\ H_2O$

[a] The possible presence of minoritary amorphous phases has not been considered in the calculation of the chemical formulae.

From these results we can confirm that the hydrotalcite R_{1080}, obtained by traditional refluxing, practically maintains the theoretical cations ratio. On the other hand, there is an important increase in the Ni/Al and Mg/Al molar ratios whereas the Ni/Mg ratio is similar for the sample $453MW_{120}$. Regarding the stoichoimetry obtained for this sample, it is possible to think that the formation of additional phases could take place, although we have not found any evidence by XRD. From the parameter mol Al/g HT obtained for both samples we can calculate % of aluminium loss expressed as g Al /100 g HT

(%). Thus, the sample $453MW_{120}$ has around 45% less of aluminium than sample R_{1080}. The cation ratios obtained could be explained because of a progressive degradation process on the sheets due to the microwaves action. Therefore, some local overheating during the microwaves treatment generates disagreggations of aluminium species in an important amount for this sample. These disaggregated aluminium species should be mainly eliminated during the washing of the gel. For the rest of the samples aged under microwaves, there is a decrease of the aluminium content but in less extension than for sample $453MW_{120}$ (Table 6). From these results we can conclude that the increase in the aging temperature and in the aging time under microwaves involves a progressive dealumination of the hydrotalcite layers. In contrast, the samples aged in a conventional oven do not show a significant dealumination even after 360 min. These results are in agreement with the nitrogen physisorption studies presented above.

- **CO_2-TPD/FT-IR studies**

In order to obtain information about the basicity of the hydrotalcites synthesized we used the CO_2-TPD technique. The CO_2-desorption profiles are similar for all samples. However, it is possible to distinguish two groups of samples with several differences. Figure 25 shows the results of the CO_2-TPD experiments of two samples that are representative of each group.

The CO_2-TPD profile of the hydrotalcite aged by conventional refluxing (R_{1080}) (Fig. 25a) is very similar to those of the samples $403MW_1$, $403MW_5$, $403MW_{15}$, $403MW_{30}$, $403MW_{60}$, $403MW_{120}$, $423MW_1$, $423MW_5$, $423MW_{15}$, $423MW_{30}$, $423MW_{60}$, $423MW_{120}$, $453MW_1$, $453MW_5$, $453MW_{15}$, RMW_{60}, RMW_{120}, RMW_{240}, RMW_{480}, R_{1080}, $403A_{120}$, $403A_{360}$, $423A_{120}$ and $423A_{360}$. Fig. 25b shows the CO_2-TPD profile of the sample $453MW_{120}$ that is representative of those of the hydrotalcites aged by microwaves at higher temperatures (453 K) and longer times (from 30 min).

UNIVERSITAT ROVIRA I VIRGILI
DISEÑO DE CATALIZADORES PARA UNA OBTENCIÓN LIMPIA DE 2-FENILETANOL
Olga Bergadà Miró
ISBN:978-84-691-0355-5/DL:T.2186-2007

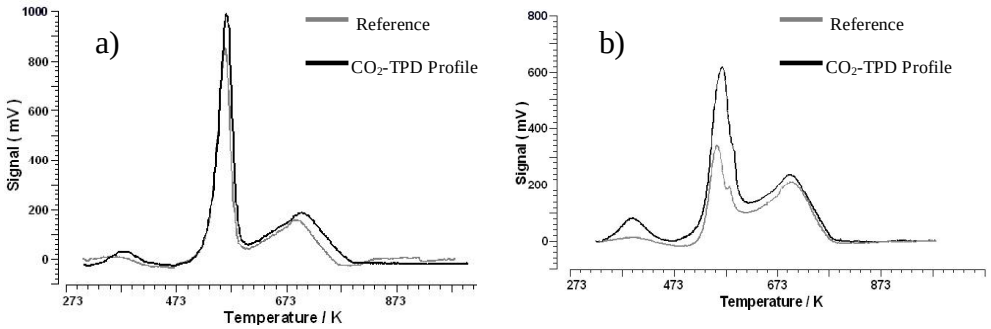

Figure 25. CO_2-TPD profiles for the samples: a) R_{1080} and b) $453MW_{120}$.

It is important to have in mind that hydrotalcites decompose with temperature and, therefore, for each sample, besides the adsorption-desorption CO_2 experiment, a thermogram was recorded without CO_2 treatment. Fig.25 also shows these decomposition thermograms for the hydrotalcites R_{1080} (Fig.25a) and $453MW_{120}$ (Fig.25b), as references. The basicity of the samples has been evaluated from the difference between the CO_2 desorption profile and the decomposition profile (reference).

Besides CO_2, other decomposition species were detected by TCD. All thermograms show three peaks. One intense and narrow at 573 K, which is related to the decomposition of carbonate observed in the reference profiles, that in the CO_2 desorption profiles is also related to CO_2 bound to basic sites. Another broader peak at 696 K is related to the formation of NO_x (identified by a mass-spectrometer) as a result of the decomposition of the nitrate at higher temperatures. Besides, a peak with low intensity appears at 398 K due to the adsorbed atmospheric CO_2 on the external surface in the reference profiles that in the CO_2 desorption profiles could also be due to some CO_2 bound to weaker basic sites.

By comparing the two reference profiles (Fig.25a and 25b), we can observe that the peak at 573 K has lower intensity in the sample $453MW_{120}$. This agrees with the loss of aluminium observed by atomic absorption for this sample. Thus, the laminas are less positively loaded. This could explain the lower amount of carbonated species observed for this sample.

All hydrotalcites show basic characteristics since we can see differences in intensity between the CO_2 desorption profile and its corresponding reference. This can be associated to the amount of CO_2 that interacts with the different basic centres of the sample. In the thermograms of the hydrotalcites aged by refluxing or by autoclaving with or without microwaves at 403 K and 423 K (e.g. Fig. 25a) we can only see a slight increase of the intensity of the peaks at 398 K and 573 K respect to those of the reference. Therefore, we can say that these samples have low amount of accessible basic sites. This behaviour was also observed for the hydrotalcites aged under microwaves at 453 K at shorter aging time (< 30 min). On the other hand, the samples aged under microwaves at 453 K but at higher aging time present higher amounts of basic sites since there is a higher difference in intensity between the CO_2 desorption profile and the reference profile (e.g. Fig.25b). Interestingly, the peak at 573 K has a shoulder at higher temperatures in the two profiles whose intensity increases, together with the intensity of the peak, after CO_2 treatment (Fig.25b). This was not observed for the rest of samples (Fig.25a). Besides, the total amount of CO_2 (subtracting the CO_2 from the reference profile) was calculated as 134.7 $\mu molCO_2$/g HT for sample R_{1080} and 452.7 $\mu molCO_2$/g HT for sample $453MW_{120}$. Therefore, the higher basicity observed, especially for the sample $453MW_{120}$, is a consequence of the dealumination that takes place during the microwaves irradiation. This is in agreement with the higher surface area of this sample.

In order to obtain more information about the nature of the basic sites, a FT-IR study was performed for the samples R_{1080} and $453MW_{120}$, as synthesized, and also after CO_2 adsorption, at the conditions commented in the Experimental section (Apartat 3.2.4). Figure 26 shows the IR spectra taken for these hydrotalcites in the range 1100-1800 cm^{-1} where the carbonate (1350-1385 cm^{-1}) and bicarbonate (≈1625 cm^{-1}) bands appear [79].

UNIVERSITAT ROVIRA I VIRGILI
DISEÑO DE CATALIZADORES PARA UNA OBTENCIÓN LIMPIA DE 2-FENILETANOL
Olga Bergadà Miró
ISBN:978-84-691-0355-5/DL:T.2186-2007

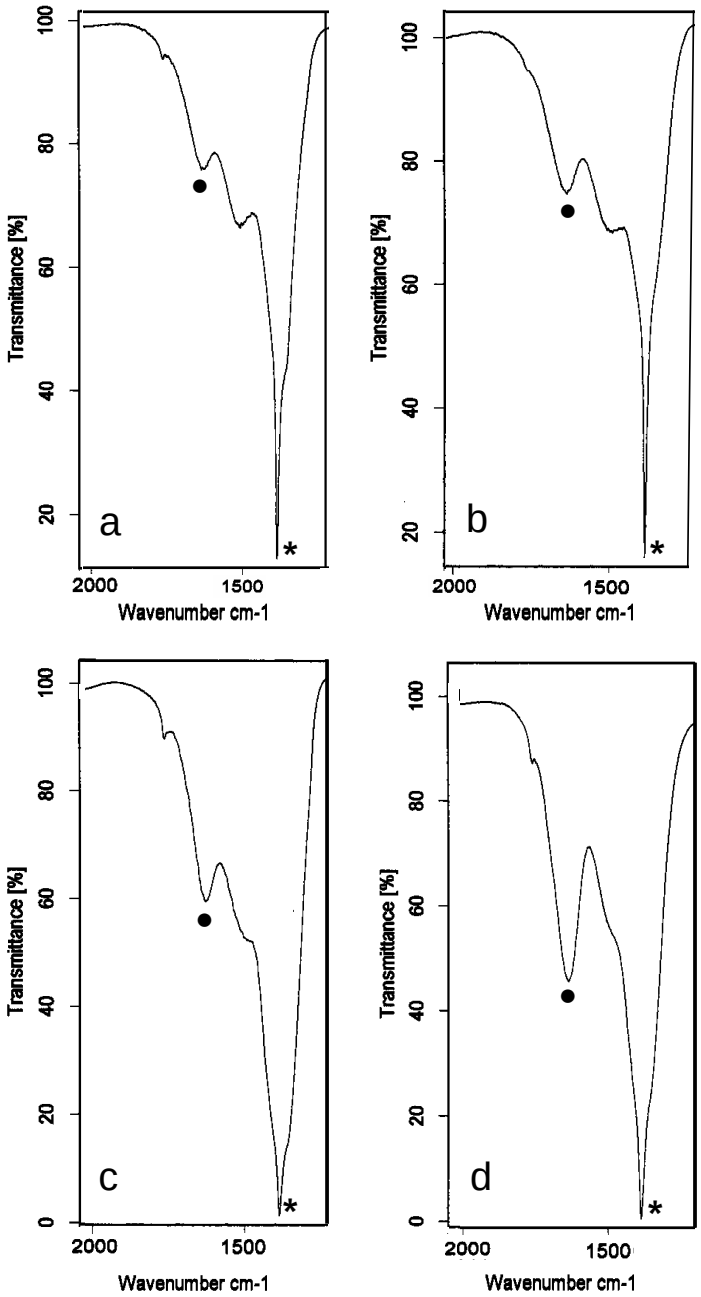

Figure 26. FT-IR of the samples: a) R_{1080} as synthesized, b) R_{1080} after CO_2 adsorption, c) $453MW_{120}$ as synthesized, and d) $453MW_{120}$ after CO_2 adsorption. Symbols: (•)bicarbonate band, and (*)carbonate band.

A different behaviour was observed when comparing the two samples. Thus, the spectrum of sample R_{1080} has a similar profile before and after CO_2 adsorption (Fig. 26a and 26b) whereas after CO_2 treatment of the hydrotalcite aged by microwaves ($453MW_{120}$) we observe a clear increase of the bicarbonate band (Fig. 26c and 26d). From these results, we can conclude that these new basic sites, associated to dealumination, are mainly OH^- that are detected as HCO_3^- species when interact with the CO_2 molecules.

- **Scanning electron microscopy (SEM) and transmission electron microscopy (TEM).**

Samples R_{1080} and $453MW_{120}$ aged without and with microwaves, respectively, were chosen as representative hydrotalcites to be studied by SEM in order to visualize possible differences in their morphologies (Fig. 27).

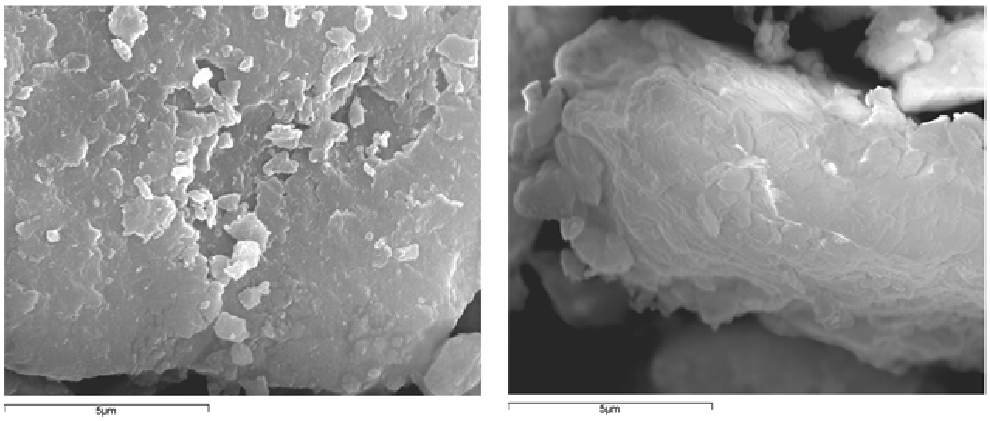

a) b)

Figure 27. SEM micrographs for the samples: a) R_{1080} (x10000) and b) $453MW_{120}$ (x10000).

For the two samples, we observe the typical hydrotalcite particles formed by superposition of sheets. However, some differences arise. The hydrotalcite aged by microwaves at higher temperature and longer time ($453MW_{120}$) has

UNIVERSITAT ROVIRA I VIRGILI
DISEÑO DE CATALIZADORES PARA UNA OBTENCIÓN LIMPIA DE 2-FENILETANOL
Olga Bergadà Miró
ISBN:978-84-691-0355-5/DL:T.2186-2007

sheets orientated in the same direction that are more defined (Fig. 27b) than those of the hydrotalcite obtained by conventional refluxing (Fig 27a).

These differences were confirmed by TEM. Fig. 28 shows the TEM micrograph taken for the sample $453MW_{120}$ where the well definition and orientation of the sheets can be observed. This is in agreement with the XRD results.

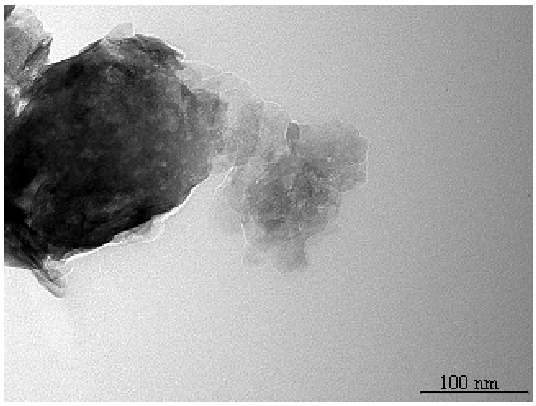

Figure 28. TEM image for the sample $453MW_{120}$.

Characterization of the most representative calcined hydrotalcites

In order to obtain information about the calcined hydrotalcites we select five hydrotalcites which are represetantive all of those synthezised. The hydrotalcites are: R_{1080}, $403MW_{15}$, $403A_{360}$, RMW_{120} and $453MW_{120}$.

XRD patterns of calcined hydrotalcites only show one crystalline phase that corresponds to NiO (Figure 29). The most crystalline NiO is that obtained from the calcination of the hydrotalcite aged in an autoclave by conventional heating ($403A_{360}C$), as confirmed by regarding its crystallite size (Table 7), whereas the less crystalline is the catalytic precursor $R_{1080}C$, whose hydrotalcite was aged by conventional refluxing. For the catalytic precursors obtained from the microwaved hydrotalcites, the most crystalline is the sample $453MW_{120}C$ whereas samples $RMW_{120}C$ and $403MW_{15}C$, whose starting hydrotalcites were aged in softer conditions, show lower NiO crystallite size values (Table 7).

Other amorphous or minority phases like MgO and Al_2O_3 were not possible to detect by this technique.

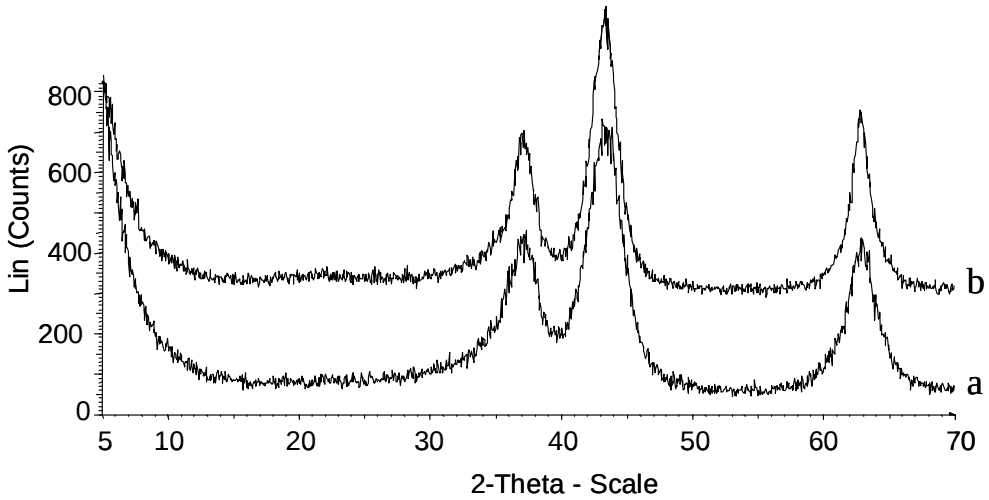

Figure 29. XRD patterns for the calcined hydrotalcites: a) $R_{1080}C$ and b) $453MW_{120}C$.

Table 7. Characterization of calcined hydrotalcites.

Sample	$R_{1080}C$	$403A_{360}C$	$RMW_{120}C$	$403MW_{15}C$	$453MW_{120}C$
Crystalline phases (XRD)	NiO	NiO	NiO	NiO	NiO
Crystallite size (nm) [a]	28	45	30	31	39
NiO/Al_2O_3 [b]	6.8	7.3	7.3	7.8	13.8
MgO/Al_2O_3 [b]	1.2	1.3	1.3	1.3	2.4
NiO/MgO [b]	5.7	5.7	5.7	5.8	5.8
BET area (m^2/g)	243	182	222	214	169
T_D(K) [c]	713	701	697	701	709
µmol CO_2/m^2 [d]	2.3	3.4	3.1	3.2	2.8

[a] Calculated from XRD results by using the Debye-Scherrer equation.
[b] Results obtained from atomic absorption.
[c] Maximum of the CO_2 desorption temperature peak.
[d] Obtained from the results of CO_2-TPD and nitrogen physisorption techniques.

UNIVERSITAT ROVIRA I VIRGILI
DISEÑO DE CATALIZADORES PARA UNA OBTENCIÓN LIMPIA DE 2-FENILETANOL
Olga Bergadà Miró
ISBN:978-84-691-0355-5/DL:T.2186-2007

From atomic absorption results, we observe that the cation ratios between Ni, Mg and Al of the calcined samples (Table 7) were found to practically correspond to those presented by their respective starting hydrotalcites (Table 6). Thus the catalytic precursor $R_{1080}C$ practically mantains the theoretical composition ratio values. Samples $403A_{360}C$, $RMW_{120}C$ and $403MW_{15}C$ present similar composition ratio values with slightly lower amount of alumina than the sample $R_{1080}C$. On the other hand, an important amount of aluminium loss, which was already detected in its starting hydrotalcite, was observed for the catalytic precursor $453MW_{120}C$ (the highest NiO/Al_2O_3 and MgO/Al_2O_3 ratios respect to the rest of samples) due to the most drastic conditions used under microwaves during the aging of its hydrotalcite precursor, as commented above. The NiO/MgO ratio practically remains constant for all samples (Table 7).

Table 7 also shows the BET area values of the calcined hydrotalcites. The decomposition process, which takes place during calcination, produces an increase in the BET area values up to 169-243 m^2/g respect to the aged hydrotalcites due to the fast release (craterisation) of H_2O, NO_x and CO_2 gases from the solid during calcination [77]. These area values can be explained taking into account the crystallinity of NiO, from XRD results, and the percentage of amorphous phases present in each sample that we know from atomic absorption results. Thus, sample $R_{1080}C$ presents the highest BET area since this is the sample with lowest crystalline NiO (smaller crystallite size) and with the highest content of amorphous Al_2O_3 (Table 7). In contrast, sample $403A_{360}C$, has the most crystalline NiO (higher crystallite size) although it has higher BET area than $453MW_{120}C$. This is due to the lowest amount of amorphous Al_2O_3 detected in this sample that, consequently, contributes with lower BET area.

CO_2 TPD profiles are similar for all calcined hydrotalcites (Fig.30). They mainly show one desorption peak whose maximum of CO_2 desorption appears at similar temperature for all samples (around 700 K) (Table 7). By comparing with the CO_2 TPD profiles of the hydrotalcites (Figs.25a and 25b), we observe that, after calcination, the peak due to NO_x disappears, as expected, whereas the peak observed in the hydrotalcites around 573 K (which was assigned to the CO_2 bound to basic sites) practically disappears and shifts to higher desorption temperatures. Also, the thermograms of the calcined hydrotalcites show a very low-intense peak around 373 K which can be mainly related to the adsorbed atmospheric CO_2 on the external surface, as observed before in the hydrotalcite samples.

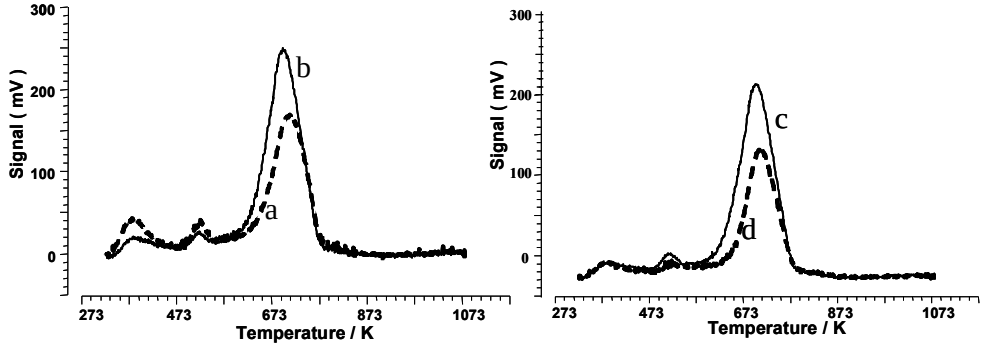

Figure 30. CO_2-TPD profiles for the calcined hydrotalcites: a) $R_{1080}C$, b) $RMW_{120}C$, c) $403MW_{15}C$ and d) $453MW_{120}C$.

Therefore, after calcination, the strength of basicity increases considerably as deduced by comparing the variation in the maxima of the desorption temperatures for each sample. This can be explained by regarding the nature of the basic sites. In the hydrotalcites, the basicity is related to the OH^- groups whereas in the calcined hydrotalcites, the basicity can be assigned to the surface O^{2-} anions [107, 111].

The calcined hydrotalcites obtained from the hydrotalcites aged under microwaves have a greater amount of basic sites by m^2 than the calcined sample obtained from the hydrotalcite aged by conventional reflux ($R_{1080}C$)

UNIVERSITAT ROVIRA I VIRGILI
DISEÑO DE CATALIZADORES PARA UNA OBTENCIÓN LIMPIA DE 2-FENILETANOL
Olga Bergadà Miró
ISBN:978-84-691-0355-5/DL:T.2186-2007

(Table 7). This is in agreement with the results reported by Corma et al. for Mg/Al oxides obtained from hydrotalcites aged under microwaves in soft conditions [107]. However, the mixed oxides obtained from the hydrotalcites prepared under microwaves in softer conditions (RMW_{120} and $403MW_{15}$) present a slightly higher amount of basic sites by m^2 than that obtained from the hydrotalcite aged under microwaves at more drastic conditions ($453MW_{120}$) (Table 7). The amorphous alumina obtained from the calcination of the hydrotalcites aged under microwaves should have some surface characteristics that could be responsible for the basicity increase. Sample $403A_{360}C$ has the highest value of basic sites by m^2. The higher NiO cristallinity and the alumina amount can explain this result.

SEM technique was used to compare the morphology of the calcined hydrotalcites $R_{1080}C$ and $453MW_{120}C$ with their hydrotalcite precursors, which were aged by conventional refluxing, and under microwaves in drastic conditions, respectively (Fig. 31). We choose these calcined hydrotalcites since their precursors are aged at very different conditions. After calcination, the two samples show particles with morphologies that remind the lamellar structure of the starting hydrotalcites. This is due to the soft calcination conditions used. Interestingly, the gases released during calcination seem to produce a different effect in the morphology of the two samples. For the sample aged by conventional refluxing, after calcination, there is an increase in the number of smaller particles due to the breaking of the hydrotalcite particles during the release of gases (Figs. 31a and 31c). In contrast, the particles of the sample $453MW_{120}C$ show an eroded appearance (Fig. 31d) when compared with those of its corresponding hydrotalcite (Fig. 27b) but practically no breaking of the particles was observed. In this case, we think that the surface-defective sites detected for the starting hydrotalcite, due to the microwaves effect, makes easy the release of gases during calcination, and consequently, a less breaking of the particles is observed. The differences in basicity detected for these samples could be related to the differences observed on their morphology.

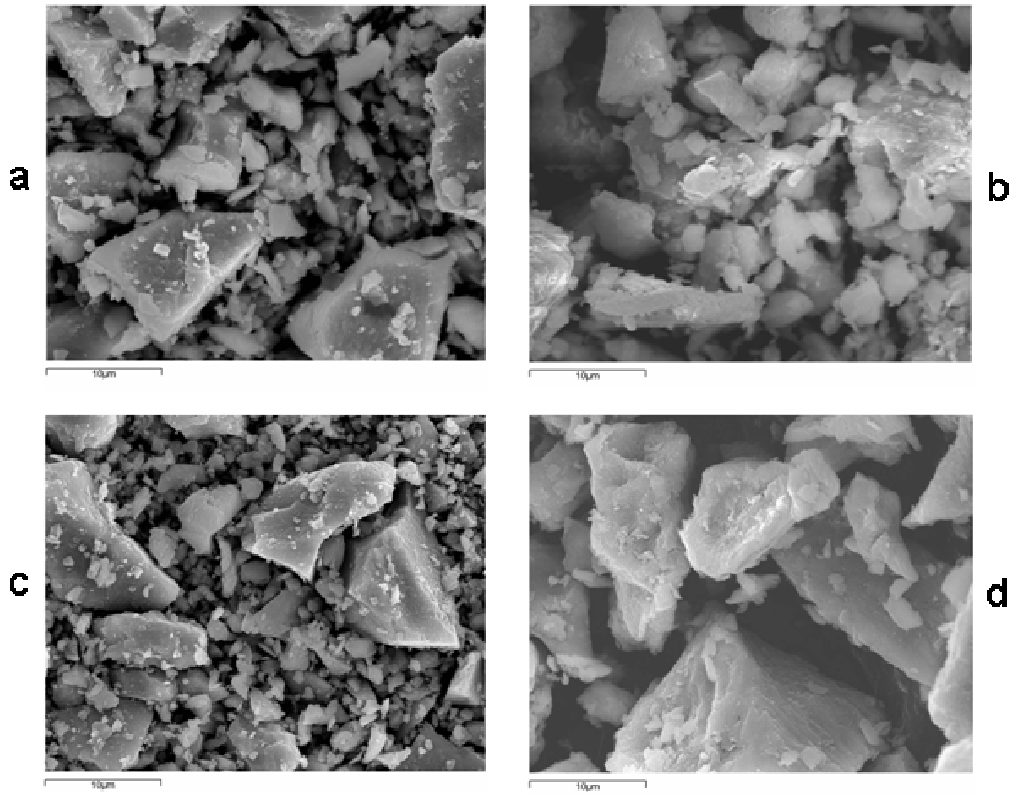

Figure 31. SEM micrographs for the samples: a) R_{1080} (x3000), b) $453MW_{120}$ (x3000), c) $R_{1080}C$ (x3000) and d) $453MW_{120}C$ (x3000).

Characterization of the catalysts

Table 8 shows some characterization data of the catalysts. After reduction of the calcined hydrotalcites, only one phase, identified as metallic nickel, was observed by XRD for all samples. Other amorphous or minority phases, like MgO and Al_2O_3, were not possible to detect again by this technique.

UNIVERSITAT ROVIRA I VIRGILI
DISEÑO DE CATALIZADORES PARA UNA OBTENCIÓN LIMPIA DE 2-FENILETANOL
Olga Bergadà Miró
ISBN:978-84-691-0355-5/DL:T.2186-2007

Table 8. Characterization of the catalysts.

Catalyst	Crystalline phases (XRD)	Metallic area (m^2/g sample)
$R_{1080}R$	Ni	26
$403A_{360}R$	Ni	25
$RMW_{120}R$	Ni	46
$403MW_{15}R$	Ni	47
$453MW_{120}R$	Ni	34

Regarding the metallic area values, the catalysts obtained from the hydrotalcites aged under microwaves ($RMW_{120}R$, $403MW_{15}R$ and $453MW_{120}R$) showed higher metallic areas than those obtained from the hydrotalcites aged in a conventional oven ($403A_{360}R$) or by conventional refluxing ($R_{1080}R$). The crystallinity of the NiO and the BET areas of the calcined hydrotalcites can explain the metallic areas obtained for their corresponding catalysts. The higher surface area of sample $R_{1080}C$ and the lowest crystallinity of its starting NiO favour the reduction process, and consequently more sintering occurs when compared with the rest of samples at the same reduction time, explaining the lower metallic area observed for catalyst $R_{1080}R$. Catalyst $403A_{360}R$ has similar metallic area than catalyst $R_{1080}R$ (Table 8) although its catalytic precursor, $403A_{360}C$, showed a more crystalline NiO and less surface area than the catalytic precursor $R_{1080}C$ (Table 7). This indicates that less sintering of the nickel particles takes place for catalyst $403A_{360}R$, because of the lower reducibility of its catalytic precursor.

On the other hand, catalysts $RMW_{120}R$ and $403MW_{15}R$ exhibit the highest metallic area values. Interestingly, their catalytic precursors have slightly lower surface areas and similar NiO crystallinity than the catalytic precursor $R_{1080}C$ (Table 7). Therefore, it seems clear that the use of microwaves during the hydrotalcite aging should favour higher metal dispersion in the final catalysts. Lastly, catalyst $453MW_{120}R$ has an intermediate value of metallic area (34 m^2/g) that is lower than those obtained for the other catalysts whose hydrotalcite precursors were aged under microwaves and higher than those

whose starting hydrotalcites were aged by conventional heating. Taking into account that this sample presents the lowest alumina content, due to the dealumination process as a consequence of the microwaves action, higher sintering of the nickel particles can be expected. From these results, we can conclude that there is a clear effect of using microwaves during hydrotalcite aging in the surface properties of the corresponding catalysts.

To obtain more information about differences in the active surface of the catalysts, the temperature-programmed desorption of hydrogen were performed for all of them. The mechanisms of adsorption-desorption of hydrogen can become extremely complex [112-117], especially over supported catalysts, because phenomena related to the interaction between the active phase and the support can interfere. The number and approximate population of the various adsorbed species depend on many factors: how the catalyst was prepared, the kind of support used and the experimental conditions of the measurement such as the weight of the sample examined, the flow rate of the carrier gas, the use of ultra-high vacuum (UHV) or the shape of the reactor system which affect conditions for removal of desorbed hydrogen.

Fig.32 shows some representative H_2-TPD profiles whereas table 9 depicts the desorption temperature at the maximum of the peaks observed for all catalysts.

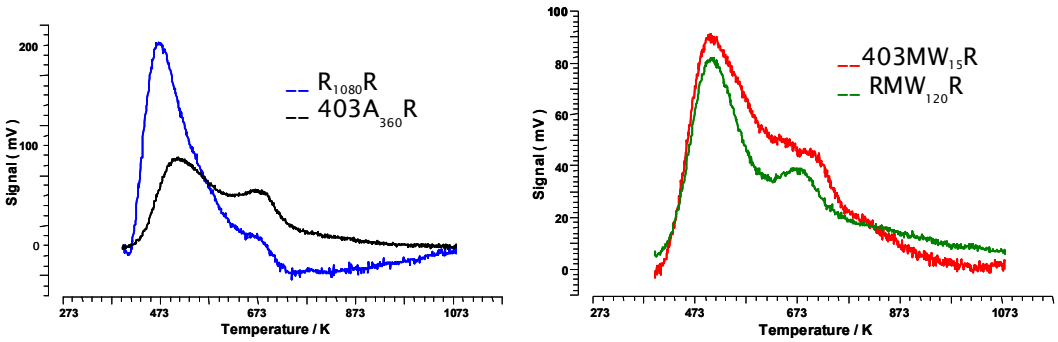

Figure 32. H_2-TPD profiles of some catalysts.

UNIVERSITAT ROVIRA I VIRGILI
DISEÑO DE CATALIZADORES PARA UNA OBTENCIÓN LIMPIA DE 2-FENILETANOL
Olga Bergadà Miró
ISBN:978-84-691-0355-5/DL:T.2186-2007

Table 9. H_2-TPD data for all catalysts.

Catalyst	T_D (K) Peak 1	T_D (K) Peak 2
$R_{1080}R$	473	-
$403A_{360}R$	513	673
$RMW_{120}R$	510	683
$403MW_{15}R$	500	703
$453MW_{120}R$	483	685

T_D (K) Maximum temperature of the desorption peak.

All H_2-TPD profiles exhibit one narrow peak with a maximum between 480 K and 515 K but with different intensities (peak 1). Catalyst $R_{1080}R$ has the most intense peak 1 (Fig. 32). Moreover, we observe another peak around 680 K (peak 2) for all catalysts except for catalyst $R_{1080}R$ (Fig.32). The H_2-TPD profile of catalyst $453MW_{120}R$ is similar to that of catalyst $403A_{360}R$ with slight higher intensity of the two peaks.

On supported-nickel catalysts [87,115,118,119], the low temperature domain of desorption, below 600 K, has been associated to different adsorption states of the hydrogen. Several authors have ascribed the high temperature peaks (above 600 K) to reverse spill-over which can take place during high-temperature (above 773 K) treatments of the catalysts [112,116]. These arguments cannot be applied for our catalysts because we used milder experimental conditions (623 K). In our case, a more probable explanation is that this high-temperature peak might be associated to other adsorption states of the hydrogen (presumably related to a different morphology, electronic properties and/or size of metal particles). We had previously observed such desorption peaks for bulk nickel and other supported nickel catalysts [87,118,119].

The different states of hydrogen observed for the catalysts will be correlated later to the activity and selectivity for the hydrogenation of styrene oxide.

Catalytic activity

Fig. 33 exhibits the catalytic activity results for all catalysts. As we can see, all catalysts show total conversion and very high selectivity to 2-phenylethanol (around 95%) at 1 hour of reaction. On the whole, we detected ethylbenzene in very low amounts (around 3 %) for all catalysts except for catalyst 403MW_{15}R that is 9% (Fig.33).

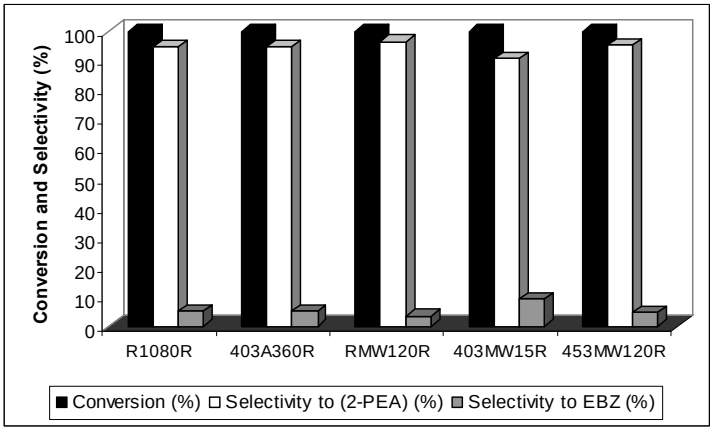

Figure 33. Catalytic activity of the catalysts after 1 hour of reaction (2-PEA = 2-phenylethanol and EBZ = ethylbenzene).

These catalytic systems based on hydrotalcites are more active than the Ni and Ni-MgO catalysts, previously tested, which were obtained from the reduction of NiO and NiO/MgO mixtures, respectively. In a previous chapter, we concluded that the presence of small nickel particles wich a certain degree of interaction with the basic sites together with low contents of available basic sites favours the activity and selectivity to 2-phenylethanol, in Ni-MgO catalysts. Thus, the higher metallic area and a more homogeneous distribution of low amounts of basic sites, when hydrotalcite precursors are used, explain their catalytic results since in these catalysts higher amounts of small nickel particles with a certain degree of interaction with the basic sites can be expected. Additionally, the use of these catalytic systems, with low amounts of oxide species, minimizes the condensation reactions, responsible for the catalyst deactivation, which were not detected in any case.

UNIVERSITAT ROVIRA I VIRGILI
DISEÑO DE CATALIZADORES PARA UNA OBTENCIÓN LIMPIA DE 2-FENILETANOL
Olga Bergadà Miró
ISBN:978-84-691-0355-5/DL:T.2186-2007

In order to explain the higher selectivity to ethylbenzene (9%) observed for catalyst $403MW_{15}R$, we have compared the H_2-TPD profiles of catalysts $403MW_{15}R$ and $RMW_{120}R$ (Fig. 32b), which have similar metallic areas (around 46 m^2/g). The H_2-TPDs of these catalysts show two peaks; the first one, appears at similar desorption temperature (around 500 K), whereas the second peak shifts to higher desorption temperature in catalyst $403MW_{15}R$ (Table 9). This can explain the presence of certain amounts of more active sites in this catalyst that could be related to its higher ethylbenzene selectivity. This is in agreement with Mitsui et al. who reported that the formation of ethylbenzene is related to the presence of more active sites [34].

More catalytic studies were performed to detect differences in the behaviour of the catalysts used. We studied the catalytic lifetime of all catalysts after reusing them ten times. The results show total conversion for catalysts $R_{1080}R$, $RMW_{120}R$ and $403MW_{15}R$ whereas for catalysts $403A_{360}R$ and $453MW_{120R}$ only 78 % of conversion was obtained (Fig.34). On the whole, the selectivity to 2-phenylethanol is maintained around 92 % except for catalyst $403MW_{15}R$ that gives to 83 % of selectivity to 2-phenylethanol.

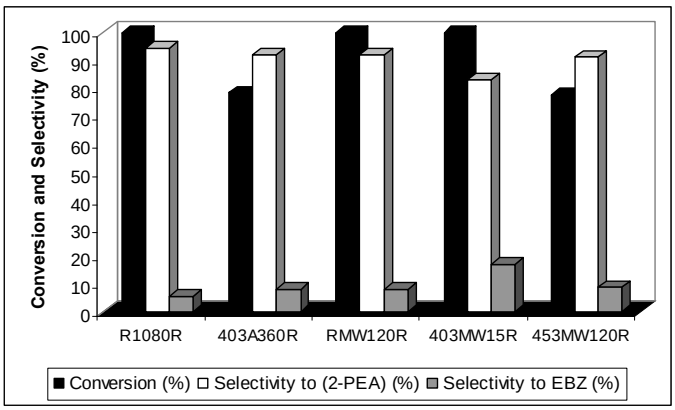

Figure 34. Catalytic lifetime of the catalysts after reusing ten times (2-PEA = 2-phenylethanol and EBZ = ethylbenzene).

The higher deactivation of catalysts $403A_{360}R$ and $453MW_{120}R$ could be understood by regarding the activity results obtained for all catalysts at

shorter reaction times. Fig. 35 shows that these two catalysts have lower conversion at shorter reaction times than the rest of catalysts although their selectivity to 2-phenylethanol is similar (85-90%).

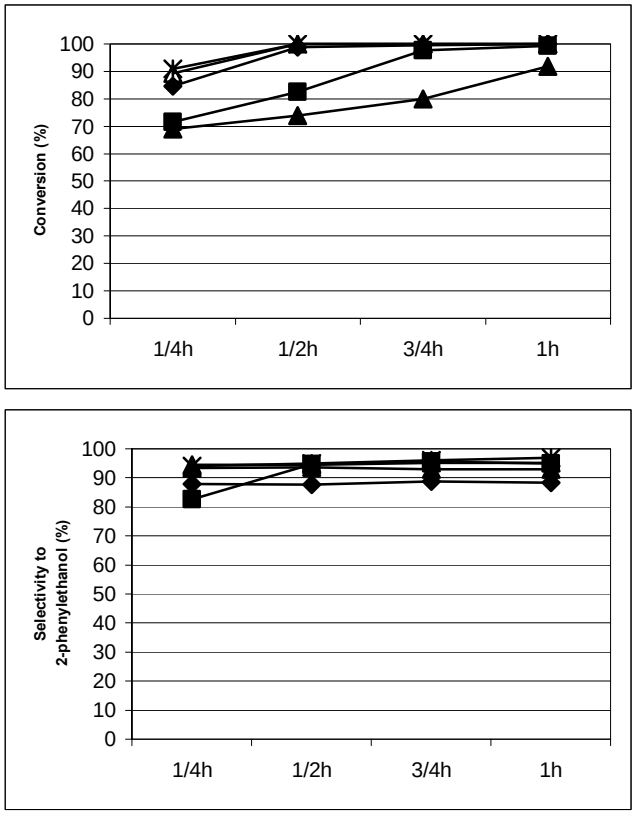

Figure 35. Catalytic activity at short reaction times for all catalysts $R_{1080}R$(⋆), $403A_{360}R$(■), $RMW_{120}R$ (△), $403MW_{15}R$(◆) and $453MW_{120}R$(▲) .

Comparing the H_2-TPDs of two catalysts ($R_{1080}R$ and $403A_{360}R$) which have similar metallic area (around 25 m^2/g, Table 2) but different activity at shorter reaction times (Fig.35), we observe that catalyst $R_{1080}R$ has a much more intense peak 1 than catalyst $403A_{360}R$ (Fig.32). Taking into account that catalyst $R_{1080}R$ is more active than catalyst $403A_{360}R$ (Fig.35), we can conclude that the hydrogen desorbed at lower temperature can be mainly related to the activity and selectivity to the desired product, 2-phenylethanol. Thus, the

UNIVERSITAT ROVIRA I VIRGILI
DISEÑO DE CATALIZADORES PARA UNA OBTENCIÓN LIMPIA DE 2-FENILETANOL
Olga Bergadà Miró
ISBN:978-84-691-0355-5/DL:T.2186-2007

presence of lower amounts of this hydrogen desorbed at lower temperature for catalysts $403A_{360}R$ and $453MW_{120}R$ can explain their lower activity and, consequently, easier deactivation.

4.2.4 Conclusions

We have confirmed that the use of microwaves during aging gives to the obtaining of hydrotalcites with higher crystallinity in shorter times than the hydrotalcites aged by conventional refluxing. Moreover, the increase of the aging temperature and the aging time favours an increase of the hydrotalcite crystallinity. Interestingly, the hydrotalcites aged in an autoclave under microwaves at the highest temperature (453 K) and at longer times (from 30 min) present new mesoporosity, higher surface area, higher basicity and higher stacking in the interlayer order than the hydrotalcites aged under microwaves in softer conditions or by traditional refluxing. These new surface properties could be related to some disaggregations of the hydrotalcite layers due to some local overheating during microwaves treatment at the conditions used for these samples. This gives to the formation of surface defective sites which are responsible for these different surface and basic characteristics.

The mixed oxides obtained by calcination of the hydrotalcites aged under microwaves in softer conditions (refluxing at 343 K for 120 min or autoclaving at 403 K for 15 min) have higher basicity by m^2 than that obtained from the hydrotalcite aged in more dractic conditions ($453MW_{120}$). This can be associated to the presence of different surface characteristics in the amorphous alumina obtained during calcination due to the effect of microwaves on their hydrotalcite precursors. The lower amount of this amorphous alumina in sample $435MW_{120}C$ justifies its lower basicity by m^2. This is corroborated by SEM since this sample presents a more eroded appearance.

The catalysts obtained from the hydrotalcites aged under microwaves showed higher metallic areas, and therefore best metal dispersion, than those

obtained from the hydrotalcites aged by conventional heating. However, the hydrotalcite aged under microwaves at hard conditions (higher temperature and time) leads to a catalyst with lower metallic area than the other microwaved samples. The lowest alumina content of this catalyst, which is due to the dealumination occurred as a consequence of the microwaves action during the hydrotalcite aging step, can explain a higher sintering of their nickel particles.

All catalysts showed total conversion and very high selectivity to 2-phenylethanol (around 95 %) after 1 h of reaction. The higher metallic area (25-47 m^2/g) and the more homogeneous distribution of low amounts of basic sites of these catalysts based on hydrotalcites when compared with other basic catalysts, as Ni-MgO systems, can explain these catalytic results. The higher amount of ethylbenzene (9 %) observed for catalyst $403MW_{15}R$ has been related to the presence of certain amounts of more active sites, as observed by H_2-TPD. After reusing ten times, all catalysts maintain high conversion and high selectivity values to 2-phenylethanol. However, catalysts $403A_{360}R$ and $453MW_{120}R$ exhibit higher deactivation than the rest of catalysts. These two catalysts also showed lower activity at shorter reaction times (< 45 min). This catalytic behaviour can be explained by the lower amount of hydrogen desorbed at lower temperatures, detected by H_2-TPD for these catalysts. Therefore, this low-temperature desorbed hydrogen can be related to the activity and selectivity to 2-phenylethanol.

UNIVERSITAT ROVIRA I VIRGILI
DISEÑO DE CATALIZADORES PARA UNA OBTENCIÓN LIMPIA DE 2-FENILETANOL
Olga Bergadà Miró
ISBN:978-84-691-0355-5/DL:T.2186-2007

4.3 Ni-Mordenite catalytic systems

4.3.1 Introduction

Mordenite is a high-silica zeolite (Si/Al > 5) characterized by its strong acidity together with size and shape selectivity. This zeolite is used in several catalytic industrial processes, including cracking and isomerization of hydrocarbons [120]. Mordenite is comprised of two 2-D straight channel types: i) larger channels, also called main channels, accessible through twelve member oxygen rings with an opening of 7.0 x 6.5 Å, and ii) smaller channels, often referred to as compressed channels which include eight member oxygen rings with 2.6 x 5.7 Å (Fig. 36). The 3-D diffusion only is possible for small molecules and the mono-dimensional diffusion is for larger molecules due to a shift among the connected channels. Each aluminum atom introduces a negative charge, counterbalanced by extraframework cations that can be located in different parts of the zeolite channels having different roles in adsorption and catalytic processes [121].

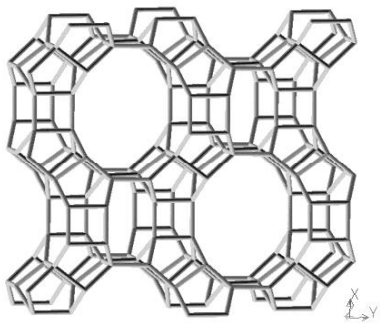

Figure 36. Structure of Mordenite

Zeolites can be modified by replacing some or all of their exchangeable cations with those of transition metals. The most used procedures to introduce cations into zeolites are impregnation and ion-exchange. The impregnation method gives to high cation concentration but it is hard to obtain regular cation dispersion [122]. Ion-exchange in zeolites is

mainly performed in the liquid phase obtaining a high initial dispersion, but for some of transition metals like Cu, Co or Ni the exchange process becomes difficult and incomplete due to an increase in the effective size of the cations in aqueous solution by hydration and/or hydrolysis [123]. In order to facilitate the diffusion of these bulky cations, an intermediate calcination step can be made between several exchange processes [124]. Solid-state ion exchange could be used as an alternative method to improve the cation exchange [125]. In this method, a mechanical mixture of the zeolite and the cation precursor is heated at relatively high temperatures and long times.

There is of increasing interest to incorporate Ni in zeolites due to the many applications that this transition metal has as catalyst in hydrogenation/dehydrogenation, hydrogenolysis [126], hydrodewaxing [127], hydrocracking and hydroisomerization reactions [128]. However, the conventional ion-exchange method in the liquid phase only gives to 40-50% of exchanged nickel, depending on the zeolite and the exchange conditions, due to the increase in the effective size of the nickel cations in aqueous solutions, as commented above [129,130].

Nowadays, microwave irradiation is being applied for chemical synthesis [96]. The use of microwaves considerably decreases the preparation times and modifies the properties of the synthesized samples when compared to those obtained by conventional heating. In the field of zeolites, microwaves have been mostly used to their dry or synthesis [131-133], and more recently, to the cation-exchange of Na^+ by La^{3+}, Co^{2+}, Cu^{2+} and Zn^{2+} in NaX and Na-ZSM-5 zeolites [134-137]. Other studies reported modifications in BrØnsted and Lewis acid centres in the X zeolite by ion-exchange of Na^+ by K^+ under microwaves heating [138]. We have not found in the literature any reference about the use of microwaves for the nickel ion-exchange of zeolites in the liquid phase. There is only one study about the solid state ion-exchange of nickel in zeolite Y under microwaves arriving to 70 % of nickel exchanged [139].

UNIVERSITAT ROVIRA I VIRGILI
DISEÑO DE CATALIZADORES PARA UNA OBTENCIÓN LIMPIA DE 2-FENILETANOL
Olga Bergadà Miró
ISBN:978-84-691-0355-5/DL:T.2186-2007

The isomerisation of styrene oxide to ß-phenylacetaldehyde is an important reaction due to the great interest of this aldehyde at industrial scale in fine chemistry for the production of fragrances, pharmaceuticals, insecticides, fungicides and herbicides [45]. This reaction is mainly catalysed by BrØnsted acid sites. In a previous work, we observed that Na-Mordenite has very low activity in the isomerization of styrene oxide whereas with H-Mordenite we obtained high selectivity to ß-phenylacetaldehyde. We also observed that the epoxide ring of styrene oxide opens mainly catalysed by both BrØnsted and Lewis acid sites [46].

In this chapter, we report a wide study of the ion-exchange of Na^+ by Ni^{2+} in a commercial mordenite under microwave irradiation in the liquid phase with the aim to achieve higher Ni^{2+} exchange degrees that can give to systems with high Ni dispersion. Some parameters, such as the salt solution concentration and volume, and the time and temperature of the exchange were modified. Besides, two samples were exchanged by conventional method for comparison. We characterized the exchanged samples by common techniques in order to study the effect of microwaves irradiation on the introduction of Ni^{2+} in the mordenite structure and on its acid properties. Four of the nickel exchanged mordenites were tested as catalysts in two reactions catalysed by different acid sites: the isomerization of styrene oxide to obtain ß-phenylacetaldehyde, which is mainly catalysed by BrØnsted acid sites, and the styrene oxide ring-opening to give 2-ethoxi-2-phenylethanol, which is catalysed by both BrØnsted and Lewis acid sites.

Moreover, the most representative samples obtained by liquid exchange, together with several samples prepared in solid state were calcined and then, reduced to obtain Ni-Mordenite catalysts. These catalysts have been tested in the hydrogenation of styrene oxide. They present acid properties and nickel distributed in the microporous support. In this new study we want to compare the catalytic behaviour of these Ni-Mordenite catalysts with the behaviour of the basic catalytic systems previously commented (Section 4.1). The competition between the hydrogenation, and the side reactions catalysed

by acid sites together with other factors associated to the microporous support will be studied.

4.3.2 Experimental

Preparation of Ni-Mordenite samples

The starting material was a commercial Na-Mordenite CBV 10A Lot No. 1822-50, designated as NaM, which was supplied by Zeolist as hydrated powder with a SiO_2/Al_2O_3 mole ratio of 6.5 and Na_2O wt % of 6.6.

- **Synthesis of HMordenite**: We prepared H-Mordenite (HM) in order to use it, later, for the synthesis of a catalyst with nickel. HM is prepared by the ion-exchange method using 1 g of NaM with 33 ml of NH_4Cl (Panreac, 99 %) 2.2 M stirred for 6 h at room temperature. Then, the sample was washed with distilled water and dried at 393 K overnight. The resulting sample was calcined at 673 K for 12 h to remove NH_3 of the sample.

Table 10 summarizes the preparation conditions for all the Ni-Mordenite samples. Commercial $Ni(NO_3)_26H_2O$ (Panreac, 99%) was used for these preparations.

- **Preparation of Ni-exchanged samples by microwaves:** We took 0.5 g of NaM for each preparation. The ion-exchanged samples prepared under microwaves were performed in an autoclave in a microwave oven (Milestone ETHOS-TOUCH CONTROL equipped with a temperature controller). The six first samples were prepared by putting NaM with 50 ml of $Ni(NO_3)_26H_2O$ 0.14M at different temperatures and times under microwaves. M1, M2 and M3 were obtained at 333 K for 15, 30 and 45 minutes, respectively, whereas M4, M5 and M6 were prepared at 353, 373 and 393 K, respectively,

UNIVERSITAT ROVIRA I VIRGILI
DISEÑO DE CATALIZADORES PARA UNA OBTENCIÓN LIMPIA DE 2-FENILETANOL
Olga Bergadà Miró
ISBN:978-84-691-0355-5/DL:T.2186-2007

for 15 minutes. Two more samples (M7 and M8) were also prepared under microwaves but by using 25 ml of $Ni(NO_3)_2 6H_2O$ 0.14 M. M7 was obtained at 333 K for 15 minutes and M8, at 393K for 15 minutes. Another block of experiments were carried out under microwaves with 50 ml of $Ni(NO_3)_2 6H_2O$ 1 M: M9 and M10 were prepared at 333 and 393 K, respectively, for 15 minutes.

Table 10. Preparation conditions of the Ni-Mordenite samples.

Nomenclature of the samples	Amount of $Ni(NO_3)_2 \cdot 6H_2O$	Exchange Time	Exchange Temperature (K)
Samples exchanged in a microwave oven			
M1	50 ml 0.14M	15 minutes	333
M2	50 ml 0.14M	30 minutes	333
M3	50 ml 0.14M	45 minutes	333
M4	50 ml 0.14M	15 minutes	353
M5	50 ml 0.14M	15 minutes	373
M6	50 ml 0.14M	15 minutes	393
M7	25 ml 0.14M	15 minutes	333
M8	25 ml 0.14M	15 minutes	393
M9	50 ml 1M	15 minutes	333
M10	50 ml 1M	15 minutes	393
Samples exchanged by conventional method			
M11	50 ml 1M	24 hours	333
M12	50 ml 1M	24 hours	298
Samples exchanged twice in a microwave oven with a thermal treatment between the exchanges			
M13	50 ml 1M	15 minutes each exchange thermal treatment in an oven at 673 K	333
M14	50 ml 1M	15 minutes each exchange thermal treatment in a microwave oven at 453 K	333
Samples prepared in solid state			
NaM-NiO	2.5 g	-	-
HM-NiO	2.5 g	-	-
NiNaM33	2.5 g	24 hours	473
NiNaM6	0.33 g	24 hours	473

- **Preparation of Ni-exchanged samples by conventional method:** To compare with the microwaved samples, two samples (M11 and M12) were exchanged by traditional ion-exchange method without microwaves by using 50 ml of $Ni(NO_3)_2 6H_2O$ 1 M. M11 was prepared at 333 K for 24 hours whereas M12 was obtained at 298 K for 24 hours.

- **Preparation of samples by two exchange processes in a microwave oven with a thermal treatment between them:** Samples M13 and M14 were exchanged twice at the same conditions than sample M9 making an intermediate thermal treatment between the two exchanges. Thus, M13 was heated in an oven at 673 K for 12 hours between the two exchange processes. This temperature was chosen taking into account the values found in the literature to improve exchange in transition metals [140]. M14 was heated between the two exchanges, in the microwave oven at 453 K for 6 hours.

- **Preparation of samples in solid state:** NiNaM33 was prepared by mixing in solid state 2.5 g of $Ni(NO_3)_2 6H_2O$ (to achieve 0.5 g of active phase after reduction step, which corresponds to 33% of Ni) with 0.5 g of NaM. The resulting mixture was placed in an oven at 343 K (melting state for $Ni(NO_3)_2 6H_2O$) for 12 hours. Then, the sample was heated in a furnace at 473 K for 24 h, in order to favour the migration of the Ni^{2+} inside the NaM. Sample NiNaM6 was prepared in the same way that sample NiNaM33 but by mixing in solid state 0.33 g of $Ni(NO_3)_2 6H_2O$ (stoichiometric amount to obtain total exchange, which corresponds to 6.4% of Ni) with 0.5 g of NaM. Finally, samples NaM-NiO and HM-NiO were prepared by stirring in cyclohexane 0.4 g of NiOB (prepared as previously commented in section 4.1) with 0.4 g of NaM or HM, respectively, in order to compare with NiNaM33 and NiNaM6.

Samples M9, M12, M13, M14, NiNaM33 and NiNaM6, were calcined at 673 K for 12 hours.

Samples M9, M12, M13, M14, NaM-NiO, HM-NiO, NiNaM33 and NiNaM6 were heated under $H_2(g)$ to be reduced in order to test their activity for the hydrogenation of styrene oxide. M9, M12, M13 and M14 were heated under

UNIVERSITAT ROVIRA I VIRGILI
DISEÑO DE CATALIZADORES PARA UNA OBTENCIÓN LIMPIA DE 2-FENILETANOL
Olga Bergadà Miró
ISBN:978-84-691-0355-5/DL:T.2186-2007

H_2(g) at 623 and 773K for 12 hours. NaM-NiO and HM-NiO were reduced at 523 K for 4 hours and NiNaM33 and NiNaM6 were reduced at 623 K for 6 hours and 12 hours, respectively. The resulting catalysts were named as M9R, M12R, M13R, M14R, NaM-Ni, HM-Ni, NiNaM33R and NiNaM6R.

Air-free sampling

The catalysts were always handled under air-free conditions after the reduction step. The catalysts were transferred in degassed cyclohexane and under hydrogen atmosphere at room temperature. The cyclohexane surface-impregnated samples were further isolated from the air with sticky tape for XRD monitoring, where a glove box was used for mounting.

Characterization of the samples

The catalytic precursors and the catalysts were characterized by X-Ray Diffraction (XRD), Nitrogen physisorption, Infrared Spectroscopy, Temperature-programmed desorption-mass spectrometry experiments (NH_3-TPD), X-Ray Microanalysis, Atomic Absorption, using model reactions to study the acid properties and Hydrogen Chemisorption. The experimental conditions used have been indicated in the Experimental Section (3.2).

Catalytic activity in the hydrogenation of styrene oxide

The catalytic hydrogenation of styrene oxide was made in the liquid phase, with NaM, HM, M9R, M12R, M13R, M14R, NaM-Ni, HM-Ni, NiNaM33R and NiNaM6R as a catalysts. We used 1 g of each catalyst, 20 ml of absolute ethanol (Panreac, 99.5%) and 4 mmol of styrene oxide (Aldrich, 97 %) with a hydrogen flow of 2 ml/s and agitation of 700 rpm. The reaction was performed at room temperature. Sample was taken each 1, 3 and 6 hour. The reaction products were analysed by gas chromatography, using a gas chromatograph Shimadzu GC-2010 instrument equipped with a 30 m capillary column DB-1 coated with phenylmethylsilicon and a FID detector.

UNIVERSITAT ROVIRA I VIRGILI
DISEÑO DE CATALIZADORES PARA UNA OBTENCIÓN LIMPIA DE 2-FENILETANOL
Olga Bergadà Miró
ISBN:978-84-691-0355-5/DL:T-2186-2007

4.3.3 Results and discussion

Characterization of the samples

- **Atomic absorption**

Figs 37, 38 and 39 show the percentage of Na^+ exchanged by Ni^{2+} obtained by atomic absorption for the M1-M14 samples.

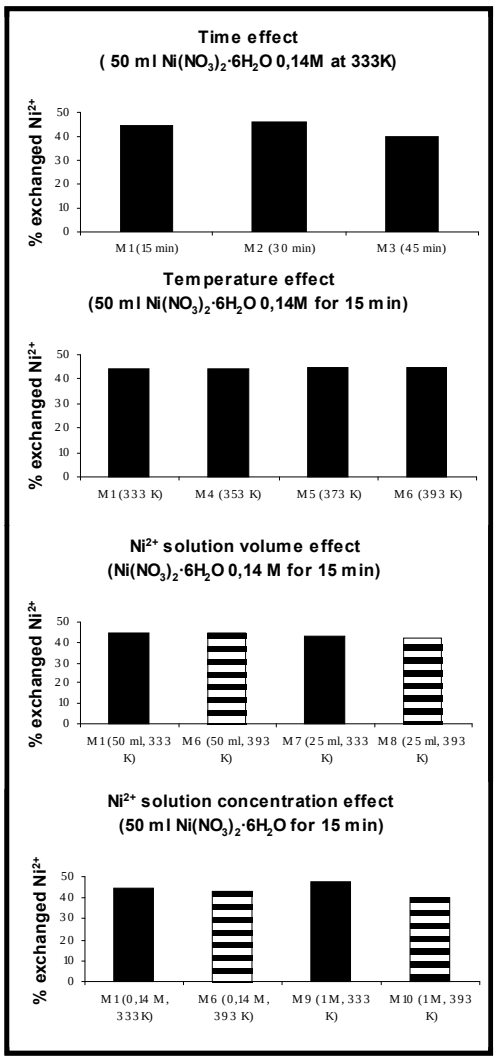

Figure 37. Exchange degree of Ni^{2+} for the samples exchanged under microwaves.

UNIVERSITAT ROVIRA I VIRGILI
DISEÑO DE CATALIZADORES PARA UNA OBTENCIÓN LIMPIA DE 2-FENILETANOL
Olga Bergadà Miró
ISBN:978-84-691-0355-5/DL:T.2186-2007

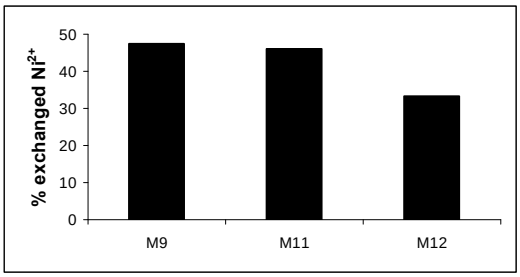

Figure 38. Exchange degree of Ni^{2+} for the samples exchanged with conventional method and by microwaves.

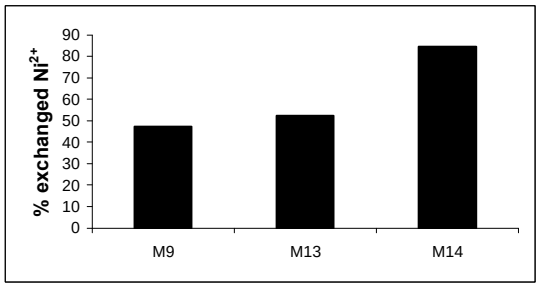

Figure 39. Exchange degree of Ni^{2+} for the samples exchanged by improving conditions.

a) Exchange under microwaves

We carried out several experiments using a microwave oven modifying different exchange variables like the temperature and time of irradiation, and the concentration and the volume of the $Ni(NO_3)_2 6H_2O$ solution in order to optimise them and achieve a high exchange degree.

We studied the effect of the exchange time at the same temperature (333 K) with the three first samples (M1, M2 and M3). The atomic absorption results show that practically there is not modification in the exchange values; even there is a slight decrease in the exchanged Ni^{2+} from 30 minutes to 45 minutes (Fig. 37). Thus, the optimum time condition is 15 minutes.

From M1, M4, M5 and M6 samples we can observe the influence of the exchange temperature (333, 353, 373 and 393 K). The results for these samples indicate that practically there is not influence of the temperature on

the exchange process at these conditions since the % of exchanged Ni^{2+} is practically the same (M1 = 44.4 % and M6 = 44.8 %) (Fig.37). So, we can choose 333 K between all the tested temperatures.

If we compare M7 with M1 and M8 with M6 (samples prepared at the same temperature but with different volume of nickel solution), we can see that the percentage of exchanged nickel is slightly higher in the samples exchanged with 50 ml of nickel solution (M1 and M6), but the values are not too much different (Fig. 37).

The last two experiments (M9 and M10) were made to investigate the influence of the nickel solution concentration with the temperature. We compared M9 with M1 and M10 with M6. An increase of the nickel solution concentration leads to an increase of the exchanged nickel at 333 K from 44.4 % to 47.4 %. In contrast, at 393 K an increase of the nickel solution concentration leads to a decrease of the exchanged nickel (from 44.8 % for M6 to 40.1 % for M10) (Fig.37).

From these results, we observe that the best exchange conditions under microwaves were found when using 50 ml $Ni(NO_3)_2 6H_2O$ 1M at 333 K for 15 minutes. However, the exchange degree obtained is lower than 50 % in all cases.

b) Exchange by conventional method

In order to compare the exchanged values obtained by using microwaves with the conventional exchange method we carried out two experiments. Samples M11 and M12 were prepared by using 50 ml of $Ni(NO_3)_2 6H_2O$ 1M for 24 hours at 333 and 298 K, respectively. The results are shown in Fig. 38. For the sample obtained at 298 K (M12) we observed the lowest Ni^{2+} exchanged value (33 %) respect to all the prepared samples whereas at 333 K (M11), the exchanged Ni^{2+} (46 %) is similar to that obtained for sample M9 (Fig 38).

UNIVERSITAT ROVIRA I VIRGILI
DISEÑO DE CATALIZADORES PARA UNA OBTENCIÓN LIMPIA DE 2-FENILETANOL
Olga Bergadà Miró
ISBN:978-84-691-0355-5/DL:T.2186-2007

The exchanged Ni^{2+} values obtained under microwaves and by conventional heating are similar, around 47 %, but, interestingly, we obtained this value 95 times faster using a microwave oven. Suzuki et al. estimated that half of the acid sites in H-Mordenite can be exchanged by nickel ions. They concluded that these exchangeable sites are situated in the main channels whereas the rest are located in side pockets, which are hardly exchangeable by the hydrated nickel ions [141].

c) Exchange improvement

In order to improve the exchanged Ni^{2+} values we carried out other experiments. Firstly, we washed with distilled water the NaM previously to the exchange process to discard problems in Ni^{2+} diffusion by the presence of species that could block the porous. Other NaM sample was submitted to two exchange processes. Each exchange was carried out with 50 ml $Ni(NO_3)_2 6H_2O$ 1M at 333 K for 15 minutes in a microwave oven and the sample was washed with distilled water and dried between the two exchange processes. The results of these two experiments did not show better exchange values.

Finally, two new experiments were performed in order to try to increase the migration of the Ni^{2+} located in the main channels, after one exchange, to the other positions less accessible of mordenite. This consists to submit the exchanged Ni^{2+} sample to a thermal treatment, to favour the cation migration, followed by a second exchange to increase the % of exchanged Ni^{2+}. For this proposal, samples M13 and M14 were prepared from commercial mordenite by exchange twice at 333 K for 15 minutes in a microwave oven (at the same exchange conditions than sample M9) with an intermediate thermal treatment between the two exchanges at 673 K in a conventional oven for 12 hours for sample M13, and an intermediate thermal treatment at 453 K in a microwave oven for 6 hours for sample M14 (Table 10). Fig. 39 shows the % of exchanged Ni^{2+} for these samples compared with sample M9. For the two new samples, we observe an increase of the Ni^{2+} content respect to M9. M13 only

shows a slight increase in the Ni^{2+} content (52 %). In fact, a grey colour due to the formation of NiO was observed for this sample after the conventional thermal step. The low increase in the Ni^{2+} content indicates that probably no diffusion of the cations occurs due to the NiO formation. On the other hand, the sample treated in a microwave oven before the second exchange (M14) has almost double content of Ni^{2+} (84 %) than the rest of prepared samples (Figs.37, 38, 39). This Ni^{2+} exchanged value is higher than those found in the literature [129,130,139]. In this case, the microwaves irradiation could favour the migration of the Ni^{2+} of the main channels to other less accessible sites of the mordenite. Some other studies pointed out that the microwave irradiation might enhance the diffusion respect to the conventional heating at the same temperature, for example, in the diffusion of various cations in Pyrex glasses [142], and ethylene oxide in polyvinyl chloride [143]. Besides, in this sample M14 more intense green colour was observed after the second exchange, confirming the higher presence of Ni^{2+}.

It is important to note that, for all the exchanged samples, we have not observed modifications of the mordenite structure or the presence of other crystalline phases by XRD. Also, IR spectra did not show dealumination of the zeolite after exchange. The calcination of the exchanged mordenites at 623 K gives to a darker grey colour but no additional crystalline phases were detected by XRD.

d) Samples prepared in solid state

The samples prepared in solid state (NiNaM33, NiNaM6, NaM-NiO and HM-NiO) were not submitted to washing treatment, so all the nickel remains in the sample. Thus, the nickel content in these samples is 44 % for NaM-NiO and HM-NiO, 33.4 % for NiNaM33 and 6.4 % for NiNaM6.

UNIVERSITAT ROVIRA I VIRGILI
DISEÑO DE CATALIZADORES PARA UNA OBTENCIÓN LIMPIA DE 2-FENILETANOL
Olga Bergadà Miró
ISBN:978-84-691-0355-5/DL:T.2186-2007

➢ Physisorption of nitrogen

All samples showed an isotherm of type I that corresponds to microporous materials. Table 11 depicts the nitrogen physisorption results of some representative exchanged mordenites respect to those of commercial Na-Mordenite (NaM). The BET area of the commercial Na-Mordenite is 380 m^2/g whereas its micropore area, obtained by the t-plot method, is 338 m^2/g. On the whole, the exchanged samples have similar BET area and similar micropore area values than commercial mordenite.

Table 11. Nitrogen physisorption results for the most representative samples.

Samples	BET Area (m^2/g)	Micropore Area (m^2/g)
NaM	380	338
M1	376	334
M9	370	323
M10	353	309
M11	378	333
M12	376	338
M13	386	342
M14	307	263
NaM-NiO	109	77
HM-NiO	103	72
NiNaM33	111	76
NiNaM6	196	151

However, sample M14, prepared by two exchanges under microwaves with an intermediate thermal treatment also under microwaves at 453 K, shows a significant lower BET area (307 m^2/g) and lower micropore area (263 m^2/g) than sample NaM. This can be explained by the higher amount of exchanged Ni^{2+} obtained for this sample (84 %) that partially blocks the entrance of the pores of the mordenite. The samples prepared in solid state show the highest decrease of the BET and micropore areas. The low surface values of samples prepared by stirring NiOB with NaM or HM (NaM-NiO and HM-NiO) can be explained by the NiO surface values contribution (50 %). In the other two

UNIVERSITAT ROVIRA I VIRGILI
DISEÑO DE CATALIZADORES PARA UNA OBTENCIÓN LIMPIA DE 2-FENILETANOL
Olga Bergadà Miró
ISBN:978-84-691-0355-5/DL:T-2186-2007

samples (NiNaM33 and NiNaM6) the amount of NiO blocking the porous of the mordenite structure explain these results. Thus, the sample with lower amount of NiO (NiNaM6) shows higher BET and micropore areas than the rest of samples prepared in solid state.

- **X-Ray microanalysis**

X-Ray microanalysis was used to confirm the Ni^{2+} exchange degree by comparing the distribution of the elements such as Al, Si, Na and Ni in one of the microwaved Ni^{2+} exchanged mordenites (M9) and in commercial mordenite. The observation of zones more and less clear in the distribution maps indicates the abundance of the element in the solid. Therefore, darker areas mean lower amount of the element. Figs. 40 and 41 show the results obtained for samples NaM and M9, respectively.

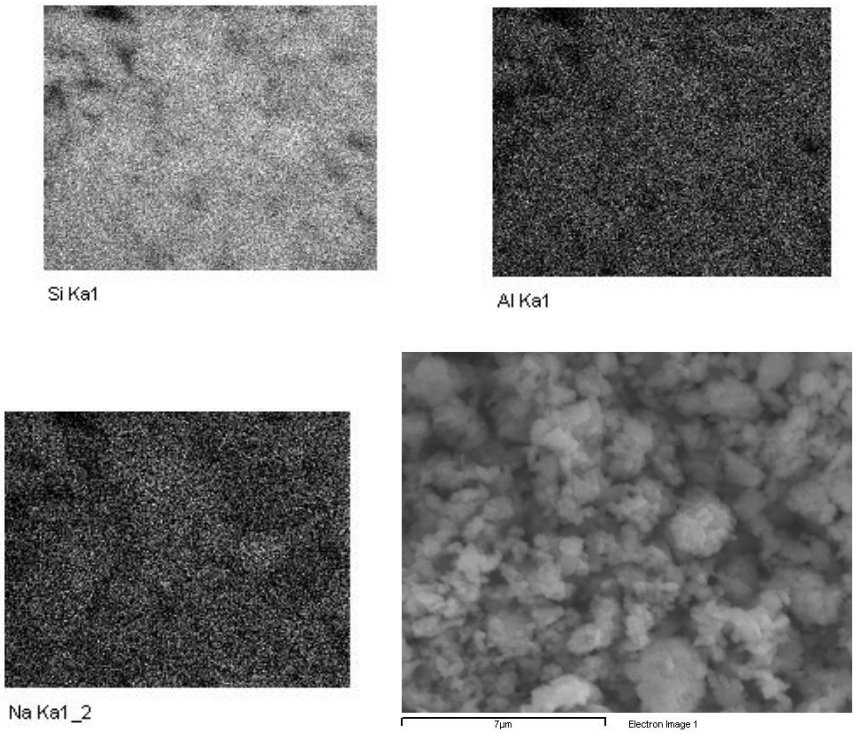

Figure 40. X-Ray microanalysis results for the sample NaM.

UNIVERSITAT ROVIRA I VIRGILI
DISEÑO DE CATALIZADORES PARA UNA OBTENCIÓN LIMPIA DE 2-FENILETANOL
Olga Bergadà Miró
ISBN:978-84-691-0355-5/DL:T.2186-2007

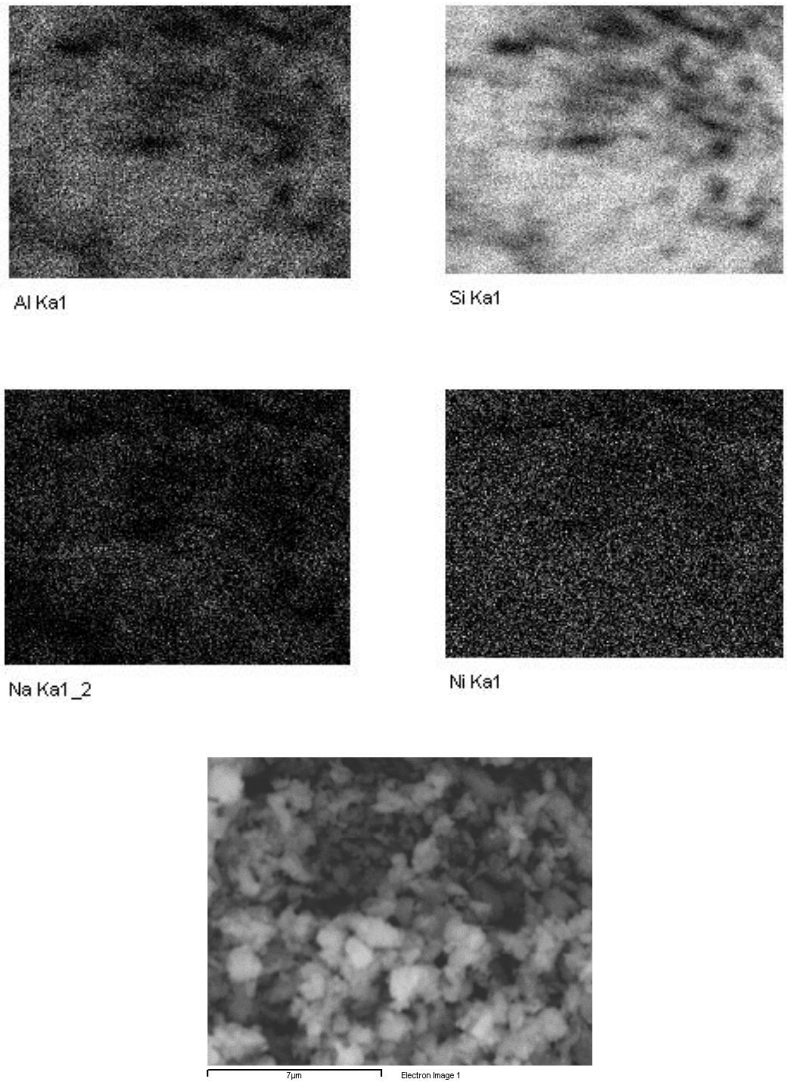

Figure 41. X-Ray microanalysis results for the sample M9.

In the two figures, we can see that the element more abundant is Si and secondly Al, as expected. From these results, we can conclude that the exchange under microwaves takes place since we observe the presence of Ni together with a decrease in the Na amount in sample M9 (Fig.41) when compared with NaM (Fig. 40).

- **Temperature-programmed desorption-mass spectrometry experiments (TPD)**

NH_3-TPD experiments were carried out in order to evaluate changes in acidity for the most representative exchanged samples (M9, M12, M13 and M14). The maxima of the desorption temperature peaks, with their relative intensities in parenthesis, are shown in table 12.

Table 12. NH_3-TPD results for some representative exchanged samples.

	NH_3 T_D (K)[a]			
Samples	**Peak 1**	**Peak 2**	**Peak 3**	**Peak 4**
NaM	-	475 (l)	-	-
M9	420 (m)	500 (h)	813 (l)	920 (m)
M12	-	513 (h)	813 (l)	933 (m)
M13	407 (h)	475 (h)	813 (vl)	871 (l)
M14	412 (h)	495 (h)	814 (vl)	-

[a] T_D: Maxima of NH_3 desorption temperature peaks.
(vl): very low-intense peak; (l): low-intense peak;
(m) medium-intense peak; (h): high-intense peak.

On the whole, we can observe four groups of desorption temperatures for the characterized samples. The first group corresponds to the desorption temperature range 407-420 K, the second group between 475-533 K, the third group corresponds to 813-814 K and the fourth group between 871-933 K. These four groups are named as peaks 1, 2, 3 and 4, respectively (table 12). When the sample exhibits peaks 1 and 2, they are partially overlapping.

The NH_3-TPD profile of Na-Mordenite only presents one peak with low intensity (peak 2) [46,144]. This peak has been assigned to ammonia weakly held or physically adsorbed on the mordenite [144]. In the rest of samples, new peaks appear at higher temperatures (peaks 3 and 4) and, consequently, different acid sites are present (Table 12). Interestingly, the samples exchanged under microwaves (M9, M13 and M14) show another peak (peak 1) which desorbs at temperatures slightly lower than peak 2. Therefore, this peak should be related to the appearance of new sites on the surface of these

UNIVERSITAT ROVIRA I VIRGILI
DISEÑO DE CATALIZADORES PARA UNA OBTENCIÓN LIMPIA DE 2-FENILETANOL
Olga Bergadà Miró
ISBN:978-84-691-0355-5/DL:T.2186-2007

samples due the microwaves action. Microwaves can give to some local overheating and favour punctual structure modifications, especially for samples M13 and M14 since they have been exposed to microwaves for a longer time. In fact, peak 1 appears more intense in these two samples. These results will be correlated later with the catalytic activity data.

- **Model reactions to study acid properties**

Four samples with different degree of exchanged Ni^{2+}, M9 (47 %), M12 (33 %), M13 (52 %) and M14 (84 %) and commercial Na-Mordenite (NaM), as a reference, were tested as catalysts in two reactions catalysed by different types of acid sites: the isomerization of styrene oxide to give ß-phenylacetaldehyde (mainly catalysed by BrØnsted acid sites) and the styrene oxide ring-opening to give 2-ethoxi-2-phenylethanol (catalysed by both BrØnsted and Lewis acid sites). We used toluene or ethanol as solvent to favour the isomerization of styrene oxide or the styrene oxide ring-opening, respectively.

a) Isomerization of styrene oxide reaction

Figure 42 shows the catalytic activity obtained for all samples. NaM has the lowest conversion. Samples M9 and M12 exhibit around total conversion whereas samples M13 and M14 present conversion values around 55-60 %. Moreover, M9 and M12 show the highest yields to ß-phenylacetaldehyde (around 90 % and 75 %, respectively) whereas for M13 and M14 samples the yield to ß-phenylacetaldehyde is around 40 %. These last two catalysts show important amounts of no identified products that have high molecular weights (named as condensation products).

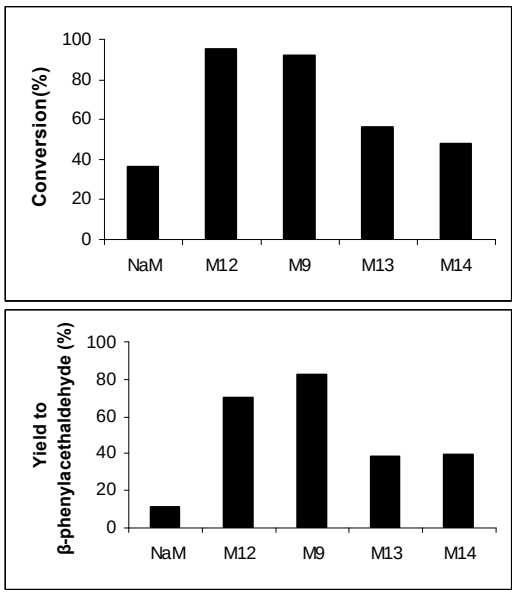

Figure 42. Catalytic activity for the isomerization of styrene oxide to ß-phenylacetaldehyde.

The higher yield values to ß-phenylacetaldehyde obtained for samples M9 and M12 can be related to the existence of BrØnsted acid sites, due to the hydrolysis of Ni^{2+}, but mainly to the presence of stronger BrØnsted acid sites, which could be associated to the effect of the proximity of the Ni^{2+} to the acid sites. The higher Ni^{2+} content of sample M9 explains its highest yield to ß-phenylacetaldehyde. However, samples M13 and M14 should have lower amount of BrØnsted acid sites due to dehydroxilation processes occurred during the intermediate thermal step for both samples. Additionally, in the case of sample M14, with the highest Ni^{2+} content, a lower amount of BrØnsted acid sites can be expected due to the presence of some agglomerations of Ni^{2+} partially blocking the entrance of the mordenite pores, as observed from the nitrogen physisorption results.

UNIVERSITAT ROVIRA I VIRGILI
DISEÑO DE CATALIZADORES PARA UNA OBTENCIÓN LIMPIA DE 2-FENILETANOL
Olga Bergadà Miró
ISBN:978-84-691-0355-5/DL:T.2186-2007

b) Styrene oxide ring-opening reaction

Figure 43 shows the catalytic activity results obtained for this reaction. Again, sample NaM shows the lowest conversion. On the other hand, the conversion is total for catalysts M9, M12 and M14 being slightly lower when using catalyst M13 (around 90 %). Catalysts M13 and M14 give to a higher yield to 2-ethoxi-2-phenylethanol (around 70 %) whereas catalysts M9 and M12 present higher amounts of condensation products and a yield to 2-ethoxi-2-phenylethanol around 40 %.

The presence of stronger Brønsted acid sites in samples M9 and M12 can explain the formation of higher amounts of condensation products. On the other hand, the presence of weaker acid sites (Brønsted and/or Lewis), some of which appeared because of the microwaves action, should explain the higher yields to 2-ethoxi-2-phenylethanol obtained for catalysts M13 and M14.

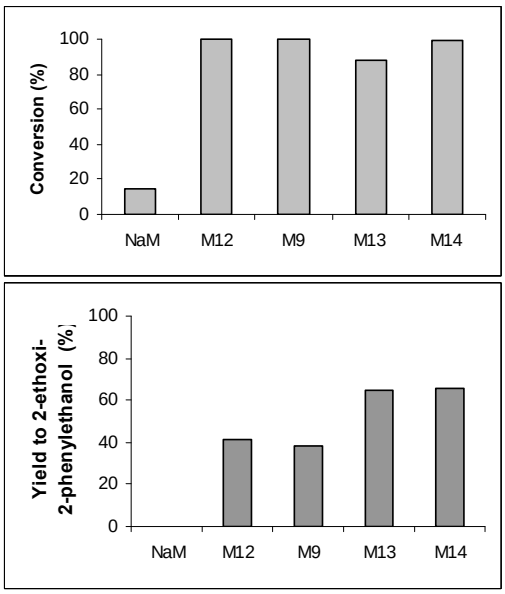

Figure 43. Catalytic activity for the styrene oxide ring-opening to 2-ethoxi-2-phenylethanol.

c) Correlation between catalytic activity and NH_3-TPD results

NH_3-TPD results of samples M9 and M12 (the catalysts with the highest yield to ß-phenylacetaldehyde in the isomerization of styrene oxide) show two peaks at high desorption temperatures (Table 12, peaks 3 and 4) with higher intensity than the rest of samples (Table 12). It is well known that the isomerization of styrene oxide to ß-phenylacetaldehyde is mainly catalysed by BrØnsted acid sites [46]. Therefore, taking into account the activity results for this reaction, peaks 3 and 4 can be assigned to BrØnsted acid sites. Besides, peak 2 can be also related to BrØnsted acid sites as deduced from the comparison with the NH_3-TPD of H-Mordenite which only present one peak at around 513 K [144].

In contrast, catalysts M9, M12, M13 and M14 show high conversion values in the styrene oxide ring-opening reaction, but only M13 and M14 give to high yields to 2-ethoxi-2-phenylethanol (Fig.43) whereas catalysts M9 and M12 give to important amounts of condensation products. The presence of stronger acid sites in catalysts M9 and M12 (Table 12, peak 4) assigned to BrØnsted acid sites, as commented above, favours the formation of these condensation products. Interestingly, the catalysts that give to high yields to 2-ethoxi-2-phenylethanol (M13 and M14) present a more intense peak 1 (Table 12). The appearance of this peak with higher intensity in the samples prepared under harder microwaves conditions, allow us to relate it to Lewis or BrØnsted acid sites associated to some modifications of the mordenite structure caused by some local overheating because of the microwaves action. Taking into account that the catalytic reactions were performed at room temperature, these weakest acid sites, assigned to peak 1, could have some effect in the catalytic activity results for this reaction. These acid sites together with the weak BrØnsted acid sites, assigned to peak 2, also present in these samples can explain the higher yield values to 2-ethoxi-2-phenylethanol obtained for catalysts M13 and M14.

UNIVERSITAT ROVIRA I VIRGILI
DISEÑO DE CATALIZADORES PARA UNA OBTENCIÓN LIMPIA DE 2-FENILETANOL
Olga Bergadà Miró
ISBN:978-84-691-0355-5/DL:T.2186-2007

- **Hydrogen Chemisorption**

Several Ni-Mordenite samples were calcined and then heated under H_2 to obtain the corresponding catalysts. These catalysts were characterized by hydrogen chemisorption in order to evaluate their metallic area.

The catalysts obtained from the samples prepared by ion exchange in a microwave oven and by conventional method (M9 and M12), and the samples prepared by two exchanges in a microwave oven with a thermal treatment between them (M13 and M14) do not show metallic areas even when using higher reduction temperatures (673 and 773 K). A possible strong interaction between the nickel cations and the mordenite structure can explain these results. Consequently, reduction does not seem to be achieved for these samples.

On the other hand, catalysts NiNaM33R and NiNaM6R have 5.7 and 1.2 m^2/g sample, respectively. The difference in the metallic areas for these samples is proportional to the nickel amount used in their preparation. The obtaining of metallic area in these samples indicate that we have obtained catalysts with metallic sites in competition with acid sites probably located in the internal surface of the support. Catalysts NaM-Ni and HM-Ni, whose precursors were prepared by mixing the phases, show very low metallic areas (< 1 m^2/g sample). The low metallic area found for the bulk nickel catalyst (NiB), commented in section 4.1 (1.7 m^2/g sample), and the contribution of mordenite amount can explain these results.

Catalytic activity for the hydrogenation of styrene oxide

Ten catalysts with different nickel content were tested in the hydrogenation of styrene oxide. Firstly, we tested samples NaM and HM without metallic phase for comparison. Then, catalysts M9R, M12R, M13R and M14R with 3.2 %, 2.3 %, 3.6 % and 5.8 % of nickel content, respectively, were tried out at the same reaction conditions. Finally, we also tested catalysts NaM-Ni and HM-Ni with 44 % of nickel amount and NiNaM6R and NiNaM33R with 6.4 % and 33.4 % of nickel amount, respectively.

UNIVERSITAT ROVIRA I VIRGILI
DISEÑO DE CATALIZADORES PARA UNA OBTENCIÓN LIMPIA DE 2-FENILETANOL
Olga Bergadà Miró
ISBN:978-84-691-0355-5/DL:T-2186-2007

NaM showed low conversion (17 %) even at 6 hours of reaction whereas sample HM exhibited total conversion from 1 hour of reaction but no hydrogenation products were detected (Fig. 44). The main product was 2-ethoxi-2-phenyltehanol (around 70 %). It seems that the acid properties of HM favour the styrene oxide ring-opening to give 2-ethoxi-2-phenylethanol. NH_3-TPD results of this sample (HM) shows a thermogram with only one peak at 513 K that has been related to weak BrØnsted acid sites [46]. The presence of these acid sites explains the high yield to 2-ethoxi-2-phenylethanol and the practically absence of condensation products. The formation of condensation products has been associated to stronger BrØnsted acid sites as commented above in the styrene oxide ring-opening reaction studies.

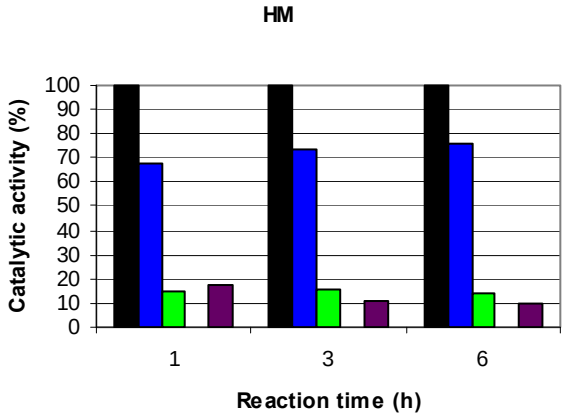

Figure 44. Catalytic activity for the sample HM.
■ Conversion (%), ■ Selectivity to 2-ethoxi-2-phenylethanol (%), ■ Selectivity to ß-phenylacethaldehyde (%), ■ Selectivity to 2-phenylethanol (%), ■ Selectivity to condensation products (%).

Figure 45 shows the catalytic activity for the catalysts obtained from the samples prepared by one exchange process (M9R and M12R). The catalytic behaviour of these two catalysts is similar. M9R and M12R show total conversion from 1 hour of reaction but the main products are 2-ethoxi-2-phenylethanol and condensation products. 2-phenylethanol or other hydrogenation products were not detected for any of these catalysts (Fig. 45a and Fig. 45b). Moreover, figure 45c and figure 45d show the yield to 2-ethoxi-

UNIVERSITAT ROVIRA I VIRGILI
DISEÑO DE CATALIZADORES PARA UNA OBTENCIÓN LIMPIA DE 2-FENILETANOL
Olga Bergadà Miró
ISBN:978-84-691-0355-5/DL:T.2186-2007

2-phenylethanol which is very similar to that obtained for their precursors, M9 and M12, at 3 hours of reaction (Fig. 43). This result is in agreement with the fact that not metallic areas were detected for these catalysts and, consequently, their catalytic behaviour must be related to the acid properties associated to Ni^{2+}. Similar values of catalytic activity were obtained when these catalysts (M9R and M12R) were reduced at higher temperatures (673 K and 773 K).

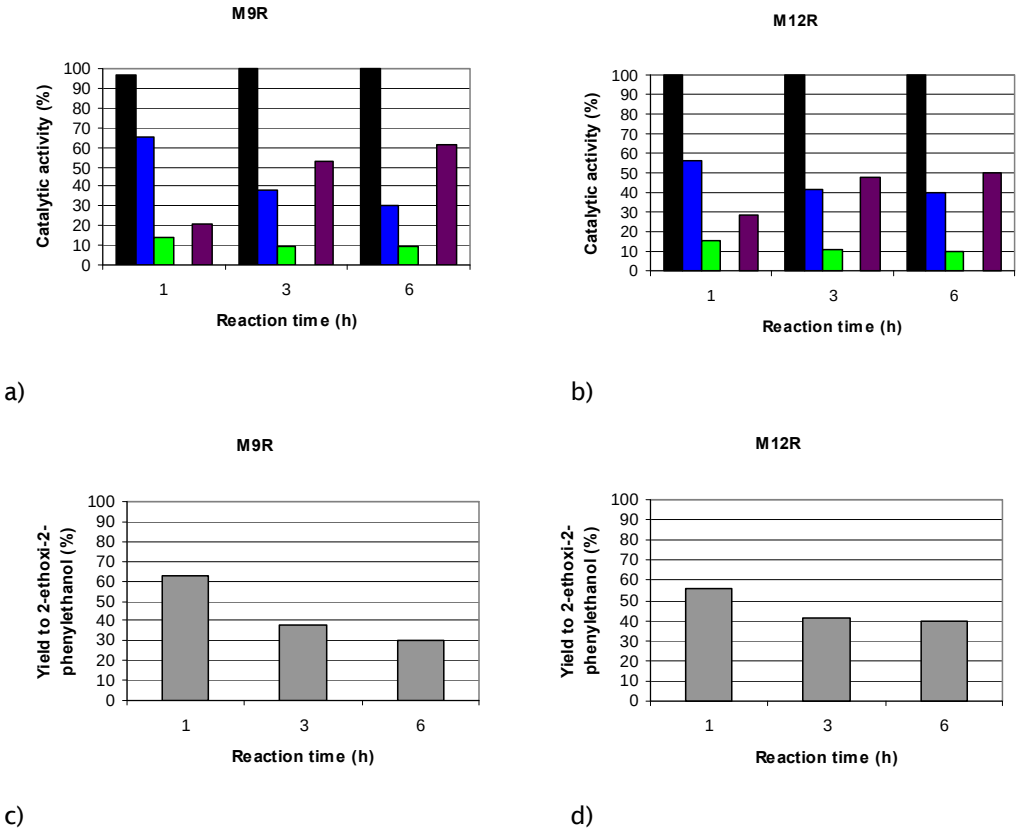

Figure 45. a) Catalytic activity for the catalyst M9R, b) Catalytic activity for the catalyst M12R, c) Yield to 2-ethoxi 2-phenylethanol for the catalyst M9R and d) Yield to 2-ethoxi 2-phenylethanol for the catalyst M12R.
■ Conversion (%), ■ Selectivity to 2-ethoxi-2-phenylethanol (%), ■ Selectivity to ß-phenylacethaldehyde (%), ■ Selectivity to 2-phenylethanol (%), ■ Selectivity to Condensation products (%), ■ Yield to 2-ethoxi-2-phenylethanol (%).

UNIVERSITAT ROVIRA I VIRGILI
DISEÑO DE CATALIZADORES PARA UNA OBTENCIÓN LIMPIA DE 2-FENILETANOL
Olga Bergadà Miró
ISBN:978-84-691-0355-5/DL:T-2186-2007

Figure 46 shows the catalytic results of the catalysts obtained from the samples exchanged twice in a microwave oven with a thermal treatment between them (M13R and M14R).

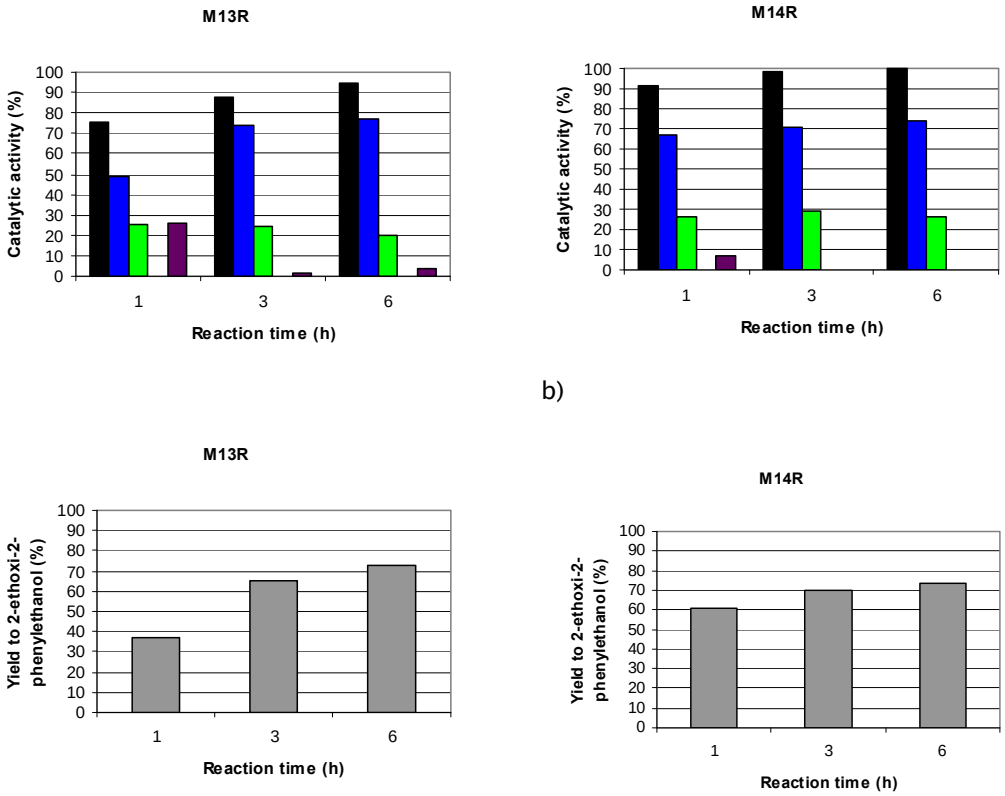

Figure 46. a) Catalytic activity for the catalyst M13R, b) Catalytic activity for the catalyst M14R, c) Yield to 2-ethoxi 2-phenylethanol for the catalyst M13R and d) Yield to 2-ethoxi 2-phenylethanol for the catalyst M14R.
■ Conversion (%), ■ Selectivity to 2-ethoxi-2-phenylethanol (%), ■ Selectivity to ß-phenylacethaldehyde (%), ■ Selectivity to 2-phenylethanol (%), ■ Selectivity to Condensation products (%), ■ Yield to 2-ethoxi-2-phenylethanol (%).

M14R shows total conversion at 6 hours of reaction whereas M13R shows 95 % of conversion at the same reaction time. However, the main products are 2-ethoxi-2-phenylethanol and ß-phenylacetaldehyde but 2-phenylethanol or other hydrogenation products are not detected for any of these catalysts (Fig 46a and Fig.46b). Moreover, figure 46c and figure 46d

UNIVERSITAT ROVIRA I VIRGILI
DISEÑO DE CATALIZADORES PARA UNA OBTENCIÓN LIMPIA DE 2-FENILETANOL
Olga Bergadà Miró
ISBN:978-84-691-0355-5/DL:T.2186-2007

shows the yield to 2-ethoxi-2-phenylethanol which is very similar to that obtained for their precursors M13 and M14 (Fig. 43). Again, this catalytic behaviour can be related to the acid properties associated to Ni^{2+} present in these samples.

Lastly, figure 47 shows the catalytic activity obtained for the catalysts prepared in the solid state.

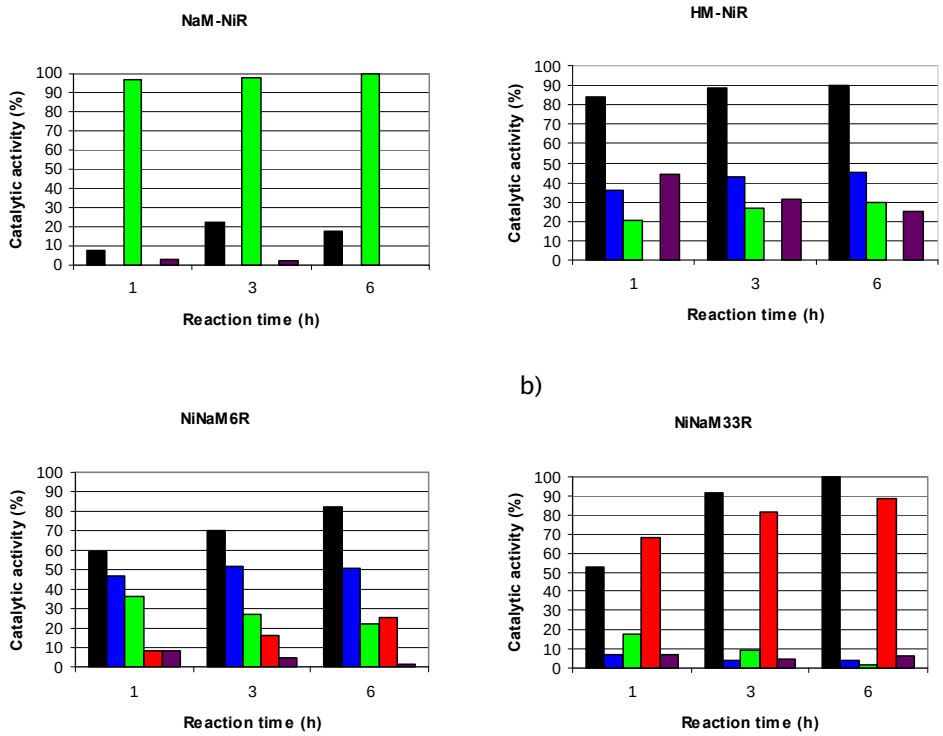

Figure 47. Catalytic activity for the catalysts prepared in solid state: a) NaM-NiR, b) HM-NiR, c) NiNaM6R and d) NiNaM33R.
■ Conversion (%), ■ Selectivity to 2-ethoxi-2-phenylethanol (%), ■ Selectivity to ß-phenylacethaldehyde (%), ■ Selectivity to 2-phenylethanol (%), ■ Selectivity to Condensation products (%).

The catalytic results of the catalysts NaM-Ni and HM-Ni, used as references, are shown in Fig. 47a and Fig. 47b, respectively. Catalyst NaM-Ni has very low activity giving to ß-phenylacethaldehyde as a main product (around 95 %), whereas catalyst HM-Ni presents higher activity (90 % of

conversion at 6 hour of reaction). We detected a mixture of reaction products for this catalyst. However, we do not detect 2-phenylethanol in any of them. It seems that the BrØnsted acid sites win in the competition between the nickel metallic sites and the BrØnsted acid sites due to the very low metallic area of these samples. The lower selectivity to 2-ethoxi-2-phenylethanol observed for catalyst HM-Ni respect to sample HM (Fig. 44) should be explained by the use of half amount of HM for its preparation.

In contrast, catalysts NiNaM6R and NiNaM33R present different catalytic activity respect to all the catalysts presented until now (Fig. 47c and 47d). At 6 hours of reaction, catalyst NiNaM6R has 80 % of conversion whereas catalyst NiNaM33R shows total conversion. On one hand, catalyst NiNaM6R gives to 2-ethoxi-2-phenylethanol and ß-phenylacethaldehyde in higher amounts, and to 2-phenylethanol and condensation products in small amounts. On the other hand, catalyst NiNaM33R shows the highest amount of 2-phenylethanol (90 % of selectivity at 6 hours of reaction). The rest of by-products observed for the other catalysts are detected in very small amounts in this catalyst.

Samples NaM-NiO, HM-NiO and NiNaM33 have similar micropore areas (Table 11) so they should have similar availability the acid sites in their corresponding catalysts. Interestingly, catalyst NiNaM33R shows the highest metallic area value (5.7 m^2/g sample) and gives to high amounts of 2-phenylethanol. Therefore, we can conclude that there is a competition between the two reactions: the hydrogenation of styrene oxide catalysed by metallic sites and the styrene oxide ring-opening catalysed by BrØnsted and Lewis acid sites. The higher amount of metallic nickel sites favours the hydrogenation of styrene oxide to give selectively 2-phenylethanol and minimize other side reactions. This also explains the fact that catalyst NiNaM6R, which has slight higher metallic area than catalysts NaM-Ni and HM-Ni but much lower metallic area than catalyst NiNaM33R, gives to small amounts of 2-phenylethanol.

UNIVERSITAT ROVIRA I VIRGILI
DISEÑO DE CATALIZADORES PARA UNA OBTENCIÓN LIMPIA DE 2-FENILETANOL
Olga Bergadà Miró
ISBN:978-84-691-0355-5/DL:T.2186-2007

4.3.4 Conclusions

We obtained around 47 % of exchanged Ni^{2+} mordenite using a microwave oven with the best conditions (50 ml $Ni(NO_3)_2 6H_2O$ 1 M at 333 K for 15 minutes). Similar values of exchanged Ni^{2+} were obtained by conventional exchanging but needing much longer time (24 hours).

Interestingly, we obtained 84 % of exchanged Ni^{2+} when we submit the sample exchanged under microwaves at the best conditions to a thermal treatment under microwaves followed by a second exchange process at the same conditions than the first exchange. This treatment could favour the migration of the nickel cations located in the main channels to other positions less accessible of mordenite. However, microwaves, especially at harder conditions, can cause some local overheating that gives to punctual modifications in the mordenite structure. This agrees with NH_3-TPD and catalytic activity results.

The exchanged Ni^{2+} mordenites present different acid properties depending on the Ni^{2+} exchange degree and the procedure used in the exchange process. The acidity has been evaluated by testing five mordenites in two reactions catalysed by different acid sites. (NaM (commercial mordenite), M9 (47 % Ni^{2+}, one exchange under microwaves), M12 (33 % Ni^{2+}, one exchange by conventional method), M13 (52 % Ni^{2+}, two exchanges under microwaves with an intermediate thermal treatment in an oven) and M14 (84 % Ni^{2+}, two exchanges under microwaves with an intermediate thermal treatment under microwaves). The catalytic behaviour of these samples has been correlated with the NH_3-TPD results. Samples M9 and M12 have higher amounts and stronger BrØnsted acid sites than the rest of samples, as observed by NH_3-TPD. This explains the high yields to ß-phenylacetaldehyde obtained in the isomerization of styrene oxide, and the important amounts of condensation products formed in the styrene oxide ring-opening reaction for these catalysts. On the other hand, the highest yields in the styrene ring-opening reaction achieved by samples M13 and M14 have been related to the

presence of weaker acid sites (peaks 1 and 2), some of which (peak 1) only appear in the samples exchanged under microwaves. These weakest acid sites only can be explained by some local overheating caused by the microwaves action that could cause some local modifications in the mordenite structure.

The catalysts obtained for the samples exchanged by microwaves or by conventional method do not show metallic areas for all reduction temperatures tested. This can be due to the strong interaction between the nickel cations with the mordenite structure. However, the catalysts obtained from the samples prepared in solid state have metallic areas.

For the hydrogenation of styrene oxide, the catalysts which become from the samples exchanged by ion exchange method (M9R, M12R, M13R and M14R) give to similar catalytic behaviour to that obtained for their precursors for the styrene oxide ring-opening (2-phenylethanol or other hydrogention products were not detected). This fact together with the null metallic areas obtained for these catalysts indicate that reduction is not achieved and similar acid sites are present. However, the catalytic activity of the Ni-Mordenite catalysts prepared in solid state (NiNaM33R and NiNaM6R) shows the formation of 2-phenylethanol which is detected in higher amounts for the catalyst with higher metallic area. This confirms that there is a competition between the styrene oxide ring-opening catalysed by acid sites and the hydrogenation of styrene oxide catalysed by metallic sites.